Reviews in Mineralogy & Geochemistry
Vol. 62, pp. 243-271, 2006



# The Stability of Hydrous Mantle Phases

**Daniel J. Frost**

*Bayerisches Geoinstitut*
*University of Bayreuth*
*D-95440 Bayreuth, Germany*
*e-mail: Dan.Frost@uni-bayreuth.de*

## INTRODUCTION

It is widely recognized that hydrous minerals are involved in a number of geochemical processes in the Earth's mantle (Michael 1988; Thompson 1992; Schmidt and Poli 1998). Their presence affects the onset of melting (Lambert and Wyllie 1968; Mysen and Boettcher 1975) and can control the partitioning of trace elements during partial melting (Adam et al. 1993; Ionov and Hoffmann 1995; La Tourrette et al. 1995; Tiepolo et al. 2000). They have accordingly been implicated in the source regions of many types of magmas including alkaline basalts and highly-potassic lavas (Edgar and Vukadinovic 1992; Foley 1992; Halliday et al. 1995; Yang et al. 2003; Elkins-Tanton and Grove 2003; Conceicao and Green 2004). As well as being intimately linked with the occurrence of mantle metasomatism (Bailey 1982; Roden and Murthy 1985), hydrous phases can also buffer fluid compositions in the mantle (Eggler 1978; Wyllie 1978) and consequently dictate the style of metasomatism. The dehydration or melting of hydrous minerals in subducting lithosphere and associated infiltration of hydrous solutions (fluids or melts) into the overlying mantle wedge are important steps in the production of island arc magmatism (Tatsumi et al. 1986; Kushiro 1987; Ulmer 2001). Conversely, the persistence of some hydrous minerals in cold regions of subduction zones may result in the transport of hydrogen into the deep mantle (Bose and Ganguly 1995; Kawamoto et al. 1995). It is therefore important to ascertain the conditions at which hydrous minerals are stable in the mantle and to recognize the situations where they breakdown and release $H_2O$. The presence of $H_2O$ in the upper mantle can lead to the production of melts that may either rise to the surface or migrate, accumulate and possibly crystallize at depth. In either case this results in chemical fractionation within the mantle.

Hydrous minerals such as amphiboles and micas are found in mantle nodules brought to the surface mainly by alkaline basalt and kimberlite lavas (Frey and Prinz 1978; Erlank et al. 1987). Most of these nodules are pieces of the subcontinental lithospheric mantle (Wilshire and Shervais 1975; Witt-Eickschen et al. 1993) although hydrous minerals are also found in nodules from the suboceanic lithosphere (Hauri et al 1993; Gregoire et al. 2000). Hydrous minerals form as a result of the interaction between the lithosphere and incoming $H_2O$-bearing melts or fluids principally from the underlying asthenosphere (Menzies et al. 1987). High pressure and temperature laboratory experiments are crucial for understanding the conditions at which such fluids or melts form, interact and crystallize in the lithosphere. Hydrous minerals don't seem to be recovered from the underlying asthenospheric mantle, which may have two reasons. 1) Melts generally arise in the top of the asthenosphere and therefore only bring samples from the overlying lithosphere. 2) Temperatures in the asthenosphere are mostly outside of the stability fields of hydrous minerals. Laboratory experiments, however, indicate that dehydration and melting temperatures of some dense hydrous minerals increase with pressure and the results of these experiments can be used to examine the likely role of hydrous minerals in $H_2O$ storage throughout the mantle.

1529-6466/06/0062-0011$05.00 DOI: 10.2138/rmg.2006.62.11

In this chapter I will address the stability of nominally hydrous minerals in the lithospheric and underlying asthenospheric/convecting mantle. The metasomatic processes that lead to the formation of hydrous minerals will be discussed, followed by a review of the types of hydrous minerals found in mantle samples from nodules and alpine peridotite massifs. The stability fields of known mantle hydrous minerals as determined by high pressure and temperature experiments will then form a foundation for a discussion of the likely stability of hydrous minerals at pressures beyond those from where xenoliths originate. These results will be used to examine the stability of hydrous minerals throughout the mantle with an emphasis on the lithosphere and what might be termed the ambient convecting mantle, as opposed to subduction zones, which are covered specifically in this volume by Kawamoto (2006).

## MANTLE METASOMATISM

Peridotite nodules from the continental Achaean lithosphere brought to the surface by kimberlites provide good evidence for the action of mantle metasomatism (Jones et al. 1982; Erlank et al. 1987). Such ultramafic xenoliths are often strongly depleted in basalt-forming major elements as a result of the removal of high temperature partial melts (O'Hara and Mercy 1963; Boyd and Mertzman 1987). They have been variably enriched, however, in some of the most incompatible trace elements, such as light rare earths, that would have been strongly depleted by melt extraction (Shimizu 1975; Hoal et al 1994). This incongruous behavior of major and trace elements is explained as the action of metasomatism, whereby a region is enriched in incompatible elements by the influx of fluids or melts (Bailey 1982; Roden and Murthy 1985; Menzies et al. 1987). The formation of new, frequently hydrous minerals as a result of the metasomatic influx is termed modal (Harte 1983) or patent (Dawson 1984) mantle metasomatism. Anhydrous minerals such as clinopyroxene, magnetite, sphene or sulfides may be also added but modal metasomatism is generally characterized by hydrous minerals. On the other hand, cryptic metasomatism is often used to describe rocks that are clearly trace element enriched but contain no obviously new metasomatic minerals.

Evidence for metasomatism is found in xenoliths from the oceanic and continental lithosphere and in a range of different volcanic settings. Dating of the enrichment processes, which can be performed using isotopic systems such as Sm/Nd and U-Pb, has shown that some events occurred in the subcontinental lithosphere a very long time ago, i.e., >1 Ga (Hawkesworth et al. 1983; Cohen et al. 1984; Kinny et al 1989; 1994). There are also examples where the timing of metasomatism in xenoliths carried by alkali basalts cannot be separated from the magmatic event that brought the samples to the surface (Menzies and Murthy 1980). The fluids or melts that caused the chemical changes are only rarely found as crystallized melts or glasses in mineral inclusions (Schrauder and Navon 1994). In some composite xenoliths and alpine massifs metasomatism can be observed in the wall rocks adjacent to veins and dikes (Jones et al. 1982; Boyd 1990; Woodland et al. 1996). Small degree melts that crystallize in the mantle and expel fluids into the wall rocks are implicated in many metasomatic events. Some alpine peridotite massifs, however, seem to have experienced phases of pervasive metasomatism over large regions, with no apparent relationship to veining (Zanetti et al. 1999; Scambelluri et al. 2006)

Metasomatism can occasionally be directly attributed to subduction zones processes, where the slab provides both fluids and a source of incompatible elements (Brandon and Draper 1996; Zanetti et al 1999; McInnes et al. 2001; Scambelluri et al. 2006). Although many metasomatized regions of the subcontinental lithosphere have not been at convergent margins for over a billion years, it is highly likely that components added by ancient subduction could be remobilized at a later date as a result of heating or decompression. In many instances metasomatism is more directly attributed to the infiltration and crystallization of small degree melts that migrate from the asthenosphere as a result of plume activity or decompression due to rifting. Menzies et al

(1987) proposed that in general terms the chemical changes that are induced in the lithosphere occur because it forms a mechanical barrier between asthenospheric melts and the surface.

A number of geochemical and laboratory based studies have addressed the nature of metasomatic agents in the mantle (Ryabchikov and Boettcher 1980; Schneider and Eggler 1986; McNeil and Edgar 1987; Bodinier et al. 1988; Gregoire et al. 2003) but it is often difficult to categorically attribute natural metasomatic assemblages to specific fluid or melt compositions. $H_2O$-rich fluids are often implicated as metasomatic agents but the conditions where they can exist in the mantle are constrained to relatively low temperatures (e.g., <900 °C between 2-3 GPa) by the $H_2O$-saturated peridotite solidus (Mysen and Boettcher 1975; Kawamoto 2004). Experiments performed at approximately 2 GPa show that $H_2O$-rich fluids in equilibrium with peridotite are poor in mafic components such as Mg, Fe and Ti and rich in Si, Na and K, with Na+K<Al (Schneider and Eggler 1986). Such fluids, however, appear to be relatively inefficient metasomatic agents as a result of relatively low solubilities and because the reactions taking place require large fluid rock ratios to actually influence element concentrations in a rock. The experiments of Adam et al. (1997) from 2 GPa indicate that hydrous fluids are also relatively inefficient at transporting and enriching trace elements when in equilibrium with peridotite rocks, particularly when compared to small degree silicate melts.

A mantle fluid phase would likely also contain C-species such as $CO_2$, CO, or at relatively reducing conditions $CH_4$. The effects of C species on the fluid present peridotite solidus vary depending on how soluble they are in silicate melts. At pressures below 2 GPa the addition of $CO_2$ to a $H_2O$ saturated system raises the peridotite solidus because $CO_2$ is more soluble in the vapor phase, which lowers the activity of $H_2O$ in the melt (Holloway 1973). At pressures above 2 GPa, however, the solidus is depressed by the addition of $CO_2$ as it becomes much more soluble in the melt phase. The peridotite solidus in the presence of $H_2O$-$CH_4$ fluids, on the other hand, is above that of the $H_2O$ saturated solidus indicating that $CH_4$ is less soluble in a melt than in a fluid phase. As $CO_2$ is added to a hydrous fluid, element solubilities go down and the fluids become peralkaline (Na+K>Al) (Schneider and Eggler 1986).

$H_2O$-$CO_2$ fluid compositions are likely to be buffered by the presence of hydrous and carbonate minerals in the mantle (Eggler 1978; Wyllie 1978). At pressures above 2 GPa the carbonates magnesite and dolomite are stable in the mantle and coexisting $H_2O$-$CO_2$ fluids will become $H_2O$-rich. Below 2 GPa carbonates breakdown and as amphiboles are stable, fluids are likely to be more $CO_2$-rich.

The association of mantle metasomatism with either fluids or silicate melts may become indistinct at high pressures because there may be no sharp division between silicate-rich fluids at lower temperature and volatile-rich silicate melts at higher temperatures (Shen and Keppler 1997; Bureau and Keppler 1999). Never the less, higher temperature hydrous silicate melts are clearly more effective metasomatic agents as they have higher solubilities of major and trace elements (Schneider and Eggler 1986; Adam et al. 1997). As will be seen in the next section there is abundant field evidence for the passage and crystallization of small degree hydrous silicate melts in the mantle.

Carbonatite melts may also be effective metasomatic agents (Wallace and Green 1988; Thibault et al. 1992; Hauri et al. 1993; Yaxley et al. 1998). Such melts that can form at pressures above 2 GPa are enriched in Na, K, Rb, Sr and P and very low in Si and high field strength elements like Ti (Wallace and Green 1988). Migrating melts would decarbonate in a reaction with enstatite at pressures below 2 GPa, releasing $CO_2$ vapor and producing clinopyroxene and olivine. The metasomatized assemblage would have higher Ca/Al and Na/Ca but as carbonatite melts have Mg/Fe ratios similar to mantle minerals the assemblage is not richer in Fe, which is counter to the effects of silicate melt infiltration as observed in some xenoliths (Yaxley et al. 1998).

Natural samples frequently show evidence for multiple generations of different metasomatic events (e.g., Woodland et al. 1996; Witt-Eickschen and Kramm 1998). From assessment of the temperature at which metasomatic events took place it is in some cases possible to make reasonable assumptions as to the types of agents involved. Scambelluri et al. (2006) for example identified two phases of metasomatism of the Ulten Zone (Eastern Italian Alps) peridotite, which likely formed part of the mantle wedge above a subduction zone. Cryptic metasomatism of spinel peridotite causing large ion lithophile and light rare earth enrichment is attributed to silicate melt percolation because it occurred at temperatures above the wet peridotite solidus. This was followed, however, by a later stage of enrichment that must have occurred at higher pressure and approximately 850 °C because hydrous minerals and garnet were formed. As this is below the wet solidus the agent was most likely an $H_2O$-rich fluid.

There is a final aspect in the definition of metasomatism that becomes very important when addressing the stability of hydrous minerals but is less important and generally ignored when the term metasomatism is used to explain source enrichment in many geochemical studies. If mantle metasomatism is considered to result from a chemical reaction between a rock, e.g., peridotite, and an incoming agent, e.g., $H_2O$-rich fluid, then the bulk composition in which a hydrous mineral forms, although the system is open, is presumably closer to that of the rock. Therefore in an experimental study on hydrous mineral stability under these conditions, a peridotite plus $H_2O$ bulk composition may be more appropriate, perhaps with the recognition that concentrations of elements such as Na, K or Ti may be raised (e.g., Mengel and Green 1989). However, it would seem that many geochemical signatures in erupted lavas that are attributed to source metasomatism i.e., that require trace element enrichment and/or residual hydrous minerals in the source (e.g., Halliday et al. 1995), could originate from partial melting of crystallized hydrous silicate melt veins or dykes in the mantle (Foley 1992). Metasomatism, in the form of wall rock reaction, is often observed around such crystallized melt veins but in some instances it is volumetrically very small or entirely absent (e.g., Woodland et al. 1996). When considering hydrous mineral stability in the veins themselves the bulk composition to be considered is that of the silicate melt. This presents a serious problem for experimental studies on the formation conditions because such veins probably do not represent crystallization from a single liquid composition but are formed instead by accumulation as melts differentiate in the mantle (Foley 1992). If the vein crystallizes without reacting significantly with wall rocks this cannot, in the petrological sense or on the scale of the vein itself, be considered to be a metasomatic event. However, when considered at the broader scale of a mantle-melting event, the crystallization of such veins without wall rock interaction is at least still metasomatism in the sense that mass transfer has occurred into the source region of melting. In this chapter there is a focus on hydrous mineral stability in peridotitic assemblages as this is the dominant rock type in the mantle. The stability of a hydrous mineral as it crystallizes from a silicate melt, however, can be quite different and several such examples of known recurrent vein compositions are discussed, such as alkaline silicate melt veins or MARID rocks. It must be appreciated, however, that a significant amount of water may be concentrated in such veins particularly in the lithospheric mantle and it is quite possible that hydrous minerals exist in deeper regions of the mantle within unknown melt vein compositions.

## EVIDENCE FROM MANTLE XENOLITHS

Hydrous mantle minerals occur in spinel peridotite xenoliths that are generally found in alkaline basalts and in garnet peridotite nodules that are more typical of kimberlite lavas. Hydrous phases are also found in ultramafic rocks from alpine type peridotite massifs. As the compositions and types of hydrous minerals vary between spinel and garnet peridotites it is helpful to consider these rock types separately.

**Peridotite massifs and xenoliths from alkaline basalts**

Two groups of ultramafic nodules have been identified from alkaline basalts, and while this classification is not all encompassing, it is useful in this context because different hydrous mineral occurrences are associated with each group. Termed group I by Frey and Prinz (1978) or Cr-diopside by Wilshire and Shervais (1975) these rocks are typical mantle peridotites, dominated by olivine with Cr-rich spinels and clinopyroxenes. These rocks have Mg# > 85 and are generally Ti-poor. They occur with a wide range of fertility from harzburgite to lherzolite and detailed studies often reveal complex histories involving melt extraction, metasomatism and reaction with the host magma during transport to the surface. Where hydrous minerals occur they are generally the calcic amphibole pargasite, (often replacing spinel), and phlogopite mica. Group II (Frey and Prinz 1978) or Al-augite rocks (Wilshire and Shervais 1975) occur as clinopyroxene dominated veins or layers in xenoliths. They are Ti-rich, Cr-poor and have Mg# < 85. They frequently contain the Ti-rich calcic amphibole kaersutite and more occasionally phlogopite. Kaersutite of similar composition can occur as monomineralic veins and is also found as megacrysts in alkaline lavas that have been interpreted as disaggregated mantle veins (Wilkinson and Le Maitre 1987).

Similar relations can be seen in alpine peridotites such as the lherz massif. Woodland et al. (1996) for example describe pyroxenite and hornblendite dikes similar to the group II/Al-augite series cross cutting spinel lherzolite. Ti-rich pargasite and kaersutite form within the dykes whereas metasomatism of the wall rocks is revealed by growth of pargasite with lesser amounts of phlogopite and a general increase in Fe content. This type of wall rock interaction that is prevalent in spinel peridotites has been termed Fe-Ti metasomatism (Menzies et al. 1987) and has been attributed to late stage crystallization of dykes and veins containing alkaline silicate melt similar to basanite. Chemical gradients develop as a response to fluid infiltration of the wall rock with zones of modal metasomatism, giving way to wider zones of trace element enrichment. As previously discussed, however, wall rock metasomatism does not always occur around such veins and in some instances the contacts with the wall rocks are sharp (Woodland et al. 1996). These relatively simple relations for spinel peridotites are not, however, without exceptions. O'Reilly and Griffin (1988) for example report Ti-poor and Ti-rich pargasite forming in both veins and wall rocks in xenoliths from Victoria, Australia. They attribute metasomatism to $CO_2$-rich fluids.

The occurrence of apatite $Ca_5(PO_4)_3(OH,F,Cl)$ in mantle rocks is also frequently attributed to $CO_2$ rich fluids or carbonatite melts (O'Reilly and Griffin 1988; Chazot et al. 1996; Woodland et al 1996). O'Reilly and Griffin (2000) argue that apatite is more widespread in lithospheric xenoliths than generally accepted as it is often overlooked or removed by acids during sample preparation. Apatite is a major host for trace elements such as Sr, Th, U and rare earths as well as P and F. O'Reilly and Griffin (2000) report that apatite found in group I type Cr diopsite lherzolites (which they term type A apatites) have significant $CO_2$ substitution (0.7-1.7 wt%) and generally higher Cl contents than F. Whereas in veins, megacryts and group II type Al-augite rocks more F-rich hydroxyl-fluor apatites (termed B-type) are found with undetectable $CO_2$ contents.

**Xenoliths from kimberlites**

Metasomatism in garnet peridotite xenoliths found in kimberlites is frequently attributed to K and $H_2O$-rich fluids as more K-rich hydrous minerals generally occur. The main hydrous mineral found is phlogopite, which is often Mg-rich and Ti-poor in comparison to its occurrence in spinel peridotites. In addition the K-rich and Al-poor amphibole K-richterite can occur and pargasitic amphiboles occur in some xenoliths. Erlank et al. (1987) recognized a series of assemblages in xenolith samples from the Kimberley cluster of kimberlites in South Africa, which they reasoned reflected increasing degrees of metasomatism of a garnet

peridotite precursor. Progressive metasomatism is documented by the replacement of garnet by phlogopite and eventually growth of K-richterite. K is introduced while Al decreases. Garnet peridotite rocks (GP) are thus succeeded by garnet phlogopite peridotites (GPP), phlogopite peridotites (PP) and ultimately phlogopite K-richterite peridotites (PKP). PKP rocks also exhibit $TiO_2$ and $Fe_2O_3$ enrichments. Similar sequences have been reported for rocks from other kimberlite localities (van Achterbergh et al. 2001). Erlank et al. (1987) estimate that garnet phlogopite peridotites (GPP), that contain ca. 1% phlogopite or less, comprise 50% of the sampled peridotite xenoliths, whereas phlogopite peridotites (PP) with over 1% phlogopite comprise 30%. Hydrous minerals also occur in veins in kimberlite peridotite xenoliths. Veins are generally dominated by phlogopite and diopside or K-richterite, phlogopite and diopside (Jones et al 1982; Erlank et al. 1987).

Another group of xenoliths that occur in kimberlite lavas worldwide are the MARID (mica-amphibole-rutile-ilmenite-diopside) suite of rocks (Dawson and Smith 1977; Wagner et al 1996). These rocks are dominated by phlogopite but compared with peridotite xenoliths, phlogopites and K-richterite amphiboles are generally higher in Fe and lower in Cr. An igneous cumulate origin for MARID rocks is often argued (Sweeney et al. 1993; Konzett et al. 1997) and several studies point to the similarity between MARID rocks and group II (orangeite) micaceous kimberlite lavas (Jones 1989; Ulmer and Sweeney 2002). It has also been proposed that the aforementioned garnet peridotite metasomatic suite described by Erlank et al. (1987) could have been formed by hydrous-fluids expelled by crystallizing MARID rocks (Jones et al. 1982; Menzies et al. 1987; Jones 1989), creating a similar relationship to group I and II xenoliths from alkaline basalts.

**Mantle amphibole mineralogy**

Even in ultramafic systems amphiboles are complex solid solutions, which contain all major elements in significant proportions. There are a number of detailed reviews of amphibole chemistry, structure and nomenclature (Thompson et al. 1981; Robinson et al. 1982; Leake et al. 1997). The standard amphibole formula is $A_{0-1}B_2C_5T_8O_{22}(OH)_2$, although in the absence of OH measurements formulae are normally reported on the basis of 23 oxygens. The important substitutions with respect to mantle amphiboles can be considered relative to tremolite $Ca_2Mg_5Si_8(OH)_2$ where the A site is vacant, Ca fills *B*, Mg is in *C* and Si in *T*. Replacing Mg and Si for 2Al constitutes the tschermakite substitution, which can be described by the exchange vector $Al_2Mg_{-1}Si_{-1}$ (Thompson et al. 1981). The edenite substitution of Na or K onto the previously vacant *A* site is accompanied by Al replacing Si ($NaAl_{-1}Si_{-1}$), whereas replacement of Ca by Na in the *B* site results in the $NaAlCa_{-1}Mg_{-1}$ glaucophane or $NaNa_{-1}Ca_{-1}$ richterite substitutions. The resulting basic amphibole classification is shown in Figure 1a with shaded boxes indicating regions that contain most mantle amphibole compositions i.e., pargasites and K-richterites. Figure 1b shows this in more detail for mantle samples in terms of (Na+K) A site occupancy and Si content. K-richterites aside, compositions from most spinel peridotite localities and alkaline basalt xenoliths cluster between pargasite and edenite but generally have a tschermakite component and occupancy of the B site by Na can be up to 40%. In addition to K-richterite, pargasite-edenite amphiboles also occur in some kimberlite xenoliths. Amphiboles in peridotite xenoliths from Jagersfontein kimberlites have been reported with compositions that span the region between pargasite and K-richterite, with some amphiboles even approaching Mg-kataphorite (Field et al. 1989). This broad compositional range may be inherited from chemical variations in the original peridotite.

In Figure 1b amphibole compositions from the Finero (Zanetti et al. 1999) and Nonsberg (Obata and Morten 1987) complexes in the Alps, which may exhibit subduction related metasomatism, show the widest scatter in compositions, whereas kaersutites have a relatively narrow compositional range. The difference between pargasitic amphiboles associated with group I (Cr-diopside) and group II (Al-augite) kaersutites, which are defined as having

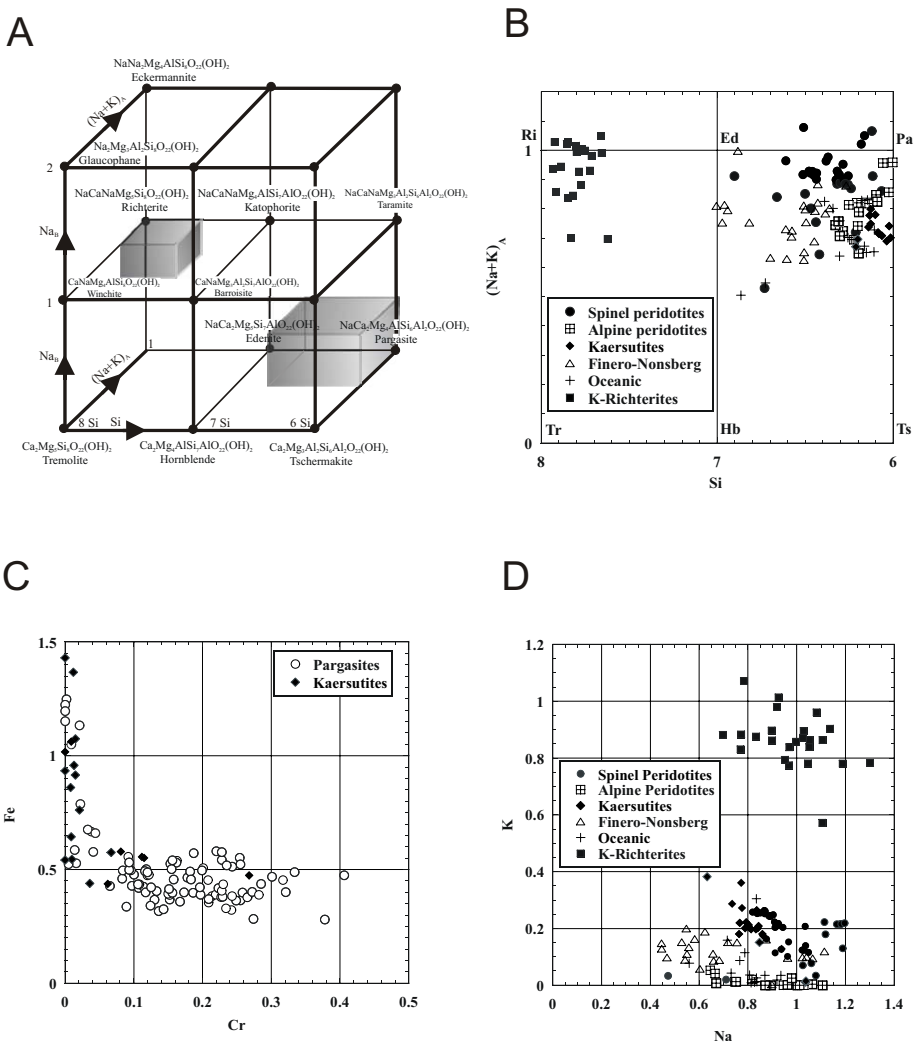


**Figure 1.** (A) Amphibole compositional space in the NCMASH system. The coordinate axes are Si formula units (which follows the tschermakite exchange vector $Al_2Mg_{-1}Si_{-1}$), Na (and K) occupancy of the A site ($NaMgAl_{-1}$) and Na in the B site ($NaAlCa_{-1}Mg_{-1}$). The compositions of mantle amphiboles generally cluster in the grey-boxed regions. (B) Mantle amphibole compositions plotted as Si formula units (23 oxygens) versus Na+K in the A site, which is a projection onto the basal plane of Figure 1A. In the legend spinel peridotites refer to xenolith samples from alkaline basalts. Finero and Nonsberg refer to peridotite bodies from the Italian Alps that may have been sections of mantle wedge. (C) Formula units of Fe versus Cr for kaersutite amphiboles from group II type xenoliths compared with low Ti pargasitic amphiboles from all localities shown in Figure 1B. (D) K versus Na contents, in formula units, of amphiboles from various localities. Amphibole compositions for all figures are from Menzies et al. (1987), Dawson and Smith (1982), Wilkinson and Le Maitre (1987), Yaxley et al. (1998), O'Reilly and Griffin (1988), Ionov (1998), Obata (1980), Seyler and Mattson (1989), Woodland et al. (1996), Fabries et al. (2001), Frey and Prinz (1978), Zanetti et al. (1999), Obata and Morten (1987), McInnes et al. (2001), Agrinier et al. (1993), Arai et al. (1997), Gregoire et al. (2000), Gregoire et al. (2003), Dawson and Smith (1977), Waters (1987), Jones et al. (1982) and Erlank et al. (1987).

more than 0.5 formula units of Ti but are otherwise similar to pargasites, can be seen in Figure 1c. In addition to higher Ti, kaersutites have generally low Cr and high Fe, which is consistent with their proposed origin as crystallizing from low degree partial melt of alkaline basalt composition (e.g., basanite). Most other amphiboles have Cr contents that are likely inherited from the protolith. Amphibole Na and K contents are shown in Figure 1d. Pargasitic amphiboles show clear differences in Na/K depending on locality whereas K-richterite compositions scatter around the general formula $KCaNaMg_5Si_8O_{22}(OH)_2$.

Studies have shown (Dyar et al. 1993; Popp et al. 1995; King et al. 1999) that Ti and $Fe^{3+}$ bearing mantle amphiboles typical of Group II type xenoliths and megacrysts are hydrogen poor as a result of oxy-amphibole substitutions such as,

$$Al^{3+} + OH^- \leftrightarrow Ti^{4+} + O^{2-} + 0.5H_2 \quad (1)$$

$$Fe^{2+} + OH^- \leftrightarrow Fe^{3+} + O^{2-} + 0.5H_2 \quad (2)$$

The substitution of higher valence cations onto the *C* site is charge balanced by the loss of hydrogen. A number of competing substitutions and the effects of closure, as discussed by Young et al. (1997), whereby two elements show correlation simply because site occupancy must add up to a constant sum, can make substitutions like (1) and (2) difficult to separate using compositional variations.

**Mantle mica mineralogy**

The biotite micas, (general formula $X_2Y_6Z_8O_{20}[OH]_4$), that occur in ultramafic xenoliths are dominated by the $K_2Mg_6[Si_6Al_2]O_{20}(OH)_4$ phlogopite end member but have up to 30% $K_2Mg_4Al_2[Si_4Al_4]O_{20}(OH)_4$ eastonite substitution, which is the mica Tschermak's component ($Al_2Mg_{-1}Si_{-1}$). Formulas are generally reported for 22 (or 11) oxygens in the absence OH measurements. Some phlogopite compositions clearly have $Al < 2$ which requires a high-Si end member that could be either the tetrasilicic mica montdorite $K_2Mg_5[Si_8O_{20}](OH)_4$ (Konzett and Ulmer 1999) or talc $Mg_6[Si_8O_{20}](OH)_4$. Phlogopites from spinel peridotite nodules show generally a greater degree of eastonite substitution than garnet peridotites. For phlogopites from garnet peridotites the eastonite component decreases with increasing degree of metasomatism (Fig. 2a) reflecting progressive Al depletion of the host rock (Erlank et al. 1987). Although in Figure 2a MARID phlogopites appear similar to those in garnet peridotites, as shown in Figure 2b phlogopites in MARIDs actually have lower Mg# (=100·Mg/[Mg+Fe]) than those from garnet peridotites. In xenoliths from alkaline basalts high Ti and low Mg# phlogopites reflect group II type vein and megacryst occurrences, whereas Mg# ca. 90 and low Ti contents are typical of group I spinel-lherzolite xenoliths. These variations can be viewed as evidence that MARID and group II rocks likely crystallized from silicate melts.

The cation sum for the octahedral (*Y*) site in biotites (i.e., $Y = Mg + Fe + Al^{VI} + Ti$ where $Al^{VI} = Al_{Total} - Al^{IV}$ and $Al^{IV} = 8 - Si$) is often less than the ideal 6, which has been attributed to vacancies in the octahedral site that balance divalent cation substitution by higher valence cations (see Fleet 2003). Al for example may substitute for Mg in the Y site with charge balance provided by the creation of a vacancy (i.e., $Al_2Mg_{-3}$). For mantle phlogopites shown in Figure 2c the octahedral cation deficit shows some correlation with Ti content, which may result from an octahedral Ti-vacancy substitution i.e., $TiMg_{-2}$ for which Trønnes et al. (1985) found evidence in experiments on Ti-rich systems. There is, in addition, evidence that mantle phlogopites range in OH concentration to values both slightly higher and significantly lower than the ideal 4. Matson et al. (1986) analyzed $H_2O$ contents of phlogopites from kimberlite xenoliths and found an excess of OH cations of over 0.5 that correlated with cation deficiency in octahedral and tetrahedral sites. This implies a similar OH substitution mechanism to some nominally anhydrous minerals. On the other hand Righter et al. (2002) report that most mantle phlogopites have a deficiency in OH that implies a relatively large oxy-component via the involvement of substitutions like Equations (1) and (2).

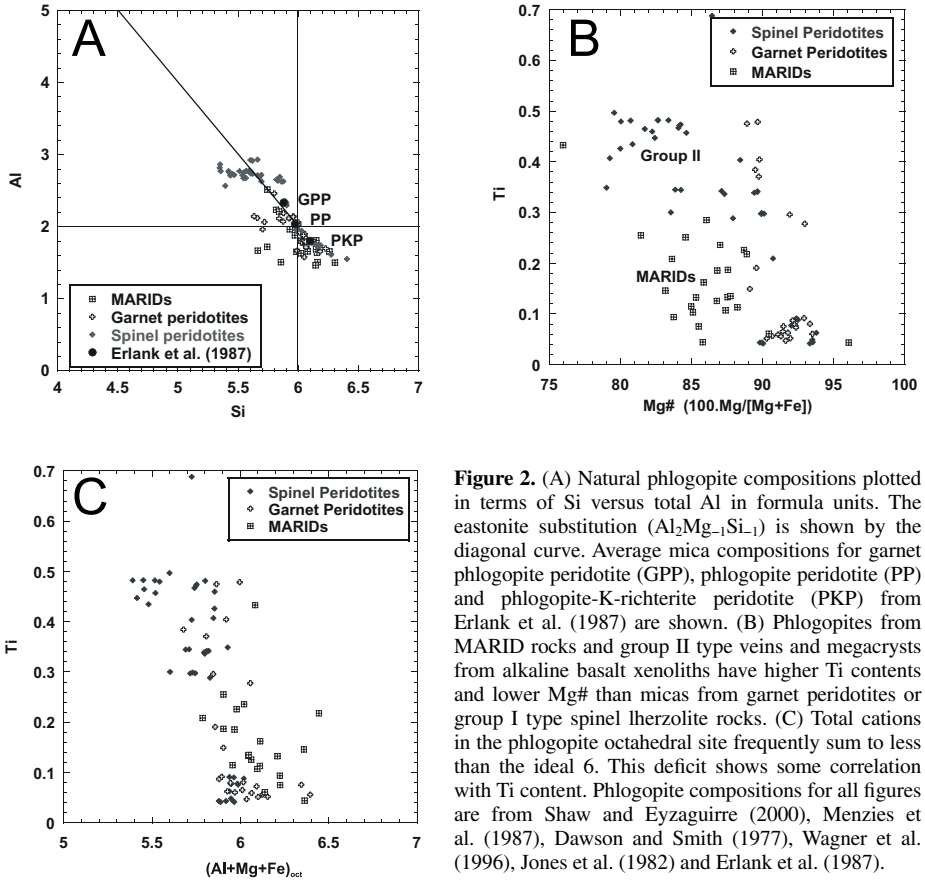


**Figure 2.** (A) Natural phlogopite compositions plotted in terms of Si versus total Al in formula units. The eastonite substitution ($Al_2Mg_{-1}Si_{-1}$) is shown by the diagonal curve. Average mica compositions for garnet phlogopite peridotite (GPP), phlogopite peridotite (PP) and phlogopite-K-richterite peridotite (PKP) from Erlank et al. (1987) are shown. (B) Phlogopites from MARID rocks and group II type veins and megacrysts from alkaline basalt xenoliths have higher Ti contents and lower Mg# than micas from garnet peridotites or group I type spinel lherzolite rocks. (C) Total cations in the phlogopite octahedral site frequently sum to less than the ideal 6. This deficit shows some correlation with Ti content. Phlogopite compositions for all figures are from Shaw and Eyzaguirre (2000), Menzies et al. (1987), Dawson and Smith (1977), Wagner et al. (1996), Jones et al. (1982) and Erlank et al. (1987).

## EXPERIMENTAL STUDIES ON THE STABILITY OF KNOWN MANTLE HYDROUS MINERALS

### Pargasitic amphiboles

There have been a significant number of experimental studies on the stability of amphiboles in simple and complex systems and over a range of water activities (see Gilbert et al. 1982). Although the experimental study of natural amphibole compositions is important, in order to identify the main factors that control amphibole stability it is often necessary to reduce the number of variables by considering simplified systems and end-members. The simplest amphibole end member relevant to ultramafic assemblages is tremolite, which has an upper thermal stability in the presence of forsterite that is controlled by the reaction:

$$\underset{amphibole}{Ca_2Mg_5Si_8O_{22}(OH)_2} + \underset{olivine}{Mg_2SiO_4} = \underset{orthopyroxene}{2.5Mg_2Si_2O_6} + \underset{clinopyroxene}{2CaMgSi_2O_6} + \underset{fluid}{H_2O} \qquad (3)$$

The equilibrium curve for this reaction is shown in Figure 3 along with stability relations of other calcic amphiboles. In comparison to tremolite, the major amphibole substitutions all lead to larger *P-T* stability fields. Jenkins (1983) showed that adding 20-30 mol% of the tschermakite component ($Ca_2Mg_3Al_2Si_6Al_2O_{22}(OH)_2$) expands the stability field by a modest amount. The coupled pargasite substitution of Na and Al, however, expands the stability field

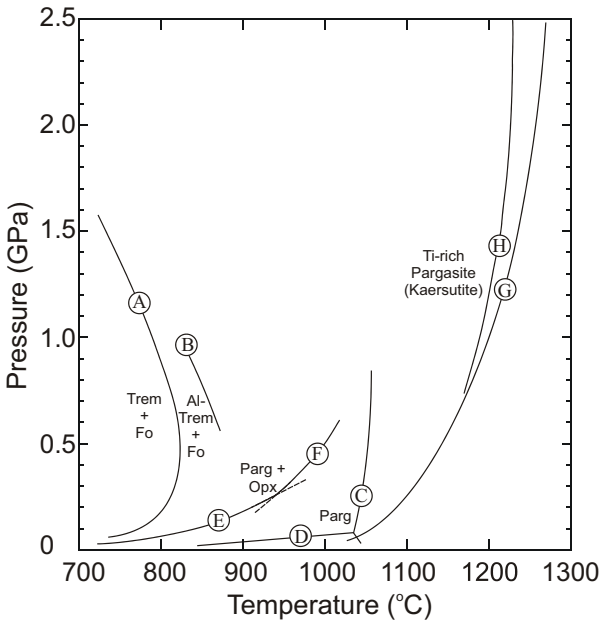


**Figure 3.** Calcic-amphibole stability relations. The curve labeled (A) is the dehydration of tremolite coexisting with forsterite via the reaction tremolite + forsterite = orthopyroxene + clinopyroxene + fluid (Jenkins 1983). (B) Dehydration of tremolite with 20-30 mol% of the tschermakite component in equilibrium with forsterite (Jenkins 1983). (C) The high temperature breakdown of pure pargasite ($NaCa_2Mg_4Al(Al_2Si_6)O_{22}(OH)_2$) by the melting reaction pargasite = clinopyroxene + forsterite + spinel + melt (Holloway 1973). (D) Low pressure breakdown of pure pargasite through the reaction pargasite = clinopyroxene + forsterite + spinel + nepheline + anorthite + fluid (Boyd 1959). (E) The breakdown of pargasite in the presence of orthopyroxene by the reaction pargasite + orthopyroxene = clinopyroxene + forsterite + plagioclase + fluid and by (F) the higher pressure reaction pargasite + orthopyroxene = clinopyroxene + forsterite + melt (Lykins and Jenkins 1992). (G) the stability of Ti-rich pargasite (magnesio-hastingsite) and (H) kaersutite (Huckenholtz et al. 1992; Merrill and Wyllie 1975). Both curves are from experiments performed on natural complex bulk compositions (K, $Fe^{3+}$ and Ti-rich magnesio-hastingsite and a kaersutite megacryst respectively). In both compositions the amphiboles breakdown above the solidus via melting reactions that involve olivine, clinopyroxene and spinel.

by over 200 as determined by Holloway (1973). Pure pargasite has a higher thermal stability than most other amphiboles and consequently its breakdown reaction at pressures above a few kilobars produces a silicate melt rather than a fluid phase. In ultramafic systems Lykins and Jenkins (1992) proposed that pargasite would breakdown in a reaction with coexisting orthopyroxene:

$$\underset{pargasite}{NaCa_2Mg_4Al_3Si_6O_{22}(OH)_2} + \underset{orthopyroxene}{2.5Mg_2Si_2O_6}$$

$$= \underset{olivine}{4Mg_2SiO_4} + \underset{clinopyroxene}{CaMgSi_2O_6} + \underset{plagioclase}{2(Na_{0.5}Ca_{0.5})(Al_{1.5}Si_{2.5})O_8} + \underset{fluid}{H_2O} \qquad (4)$$

The bracketed equilibrium curve for this reaction is shown in Figure 3.

The thermal stability of pargasitic amphiboles is further increased by the addition of Ti to produce kaersutite, which has the ideal formula $NaCa_2Mg_4TiSi_6Al_2(O+OH)_{24}$. Experiments on kaersutite have generally been performed in complex systems, such as natural kaersutite megacrysts or alkaline basalts, where Ti and $Fe^{3+}$ may both act to increase the thermal stability

(Huckenholz et al. 1992; Merrill and Wyllie 1975). Kaersutites breakdown via melting reactions that generally involve olivine, clinopyroxene and spinel. The significant hydrogen deficiency caused by the oxy-substitution involving the high field strength Ti and $Fe^{3+}$ ions in natural kaersutites (hence the sum of O+OH to 24 in the formula) can also help to explain their high thermal stability. Popp et al. (1995) performed experiments on a natural kaersutitic amphibole under controlled $P$, $T$ and hydrogen fugacity ($f_{H_2}$) up to 1 GPa and 1200 °C and determined the equilibrium constant ($K$) for amphiboles undergoing dehydrogenation by Equation (2). Using the expression for $K_{(P,T)}$ and measurements of the OH content and ferric/ferrous ratio it is therefore possible to make a calculation of the $f_{H_2}$ under which a natural sample equilibrated. If the equilibrium oxygen fugacity can be also estimated using an oxy-thermobarometer (e.g., Bryndzia and Wood 1990) then the equilibrium water activity ($a_{H_2O}$) can be determined. Mysen et al. (1998) used a kaersutite inclusion in an SNC meteorite of likely Martian origin to estimate that it crystallized from a melt with only 100-1000 ppm $H_2O$. A recurrent question, however, is whether low H contents reflect crystallization conditions or if the dehydrogenation reaction, Equation (2), occurs mainly during ascent and cooling of the xenolith. Dyar et al. (1993) argued that hydrogen diffusivity would be too slow for significant dehydrogenation to occur during ascent, while Popp et al. (1995) reasoned that a rock or melt containing amphibole would be more likely to reduce during closed system cooling and would, therefore, not undergo dehydrogenation. King et al. (1999) and Miyagi et al. (1998), on the other hand, recognized a correlation between amphibole H-content and xenolith ascent rate, whereby amphiboles from rapidly cooled rocks have higher H-contents, but slower cooled rocks have lower and more scattered values. Some natural amphiboles have such low H contents (Dyar et al. 1993; King et al. 1999) that it is difficult to understand why these amphiboles were stable with respect to an anhydrous assemblage if these compositions reflect crystallization conditions.

In addition to the chemical composition, the activity of $H_2O$ plays a key role in the stability of amphiboles, as with any hydrous mineral. At the relatively low temperatures at which an amphibole such as tremolite dehydrates the resulting fluid will be relatively pure $H_2O$. Lowering the activity of $H_2O$ in the fluid, by adding $CO_2$ for example, will decrease the high temperature stability of tremolite, which is, therefore, at a maximum in the presence of a pure $H_2O$ fluid. Pargasitic and kaersutitic mantle amphiboles, however, are stable at temperatures above the $H_2O$-saturated silicate solidus and the melting reactions that control their stability are, therefore, displaced to lower temperatures with increasing $H_2O$ activity. Contrary to the tremolite thermal stability range, the maximum thermal stability of these amphiboles occurs under fluid-absent conditions (i.e., $P_{H_2O} < P_{total}$). For the same reason experiments saturated in $H_2O$-$CO_2$ fluids below 1 GPa (Holloway 1973) show that pargasite thermal stability increases as $H_2O$ activity in the vapor phase decreases (Fig. 4). This is because the $H_2O$ activity in the coexisting melt phase is also decreasing, with the maximum thermal stability occurring where the $H_2O$ activity of the silicate melt is similar to that which occurs at the onset of vapor free melting. Whereas increasing $CO_2/H_2O$ ratio of the fluid expands the pargasite stability field in the low-pressure, fluid-saturated experiments of Holloway (1973), the increased $CO_2$ solubility in silicate melts at pressures above 2 GPa lowers the melting temperature with increasing $CO_2/H_2O$ ratio at 2-3 GPa (Wallace and Green 1988), and thus destabilizes pargasite. Under more reducing conditions, however, increasing the $CH_4$ content of a C-O-H fluid phase raises the solidus temperature, as a result of lowering the melt $H_2O$ activity, causing the amphibole stability field to expand relative to pure $H_2O$ saturated conditions (Taylor and Green 1988).

A number of studies have examined amphibole stability under vapor absent and vapor present conditions using different peridotite bulk compositions (Kushiro 1970; Green 1973; Millhollen et al. 1974; Mysen and Boettcher 1975; Mengel and Green 1989; Wallace and Green 1991; Niida and Green 1999). Figure 5 shows the amphibole stability field for 4 peridotite compositions at vapor absent conditions with the stability field for Hawaiian Pyrolite (HPY-0.2%; where 0.2% is the bulk $H_2O$ content by weight) also indicated at water saturated

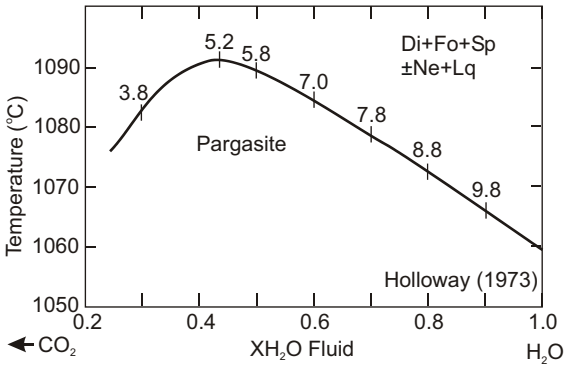


**Figure 4.** The melting of pargasite amphibole as a function of $H_2O$ content of a coexisting $H_2O$-$CO_2$ fluid. With decreasing $H_2O$ content of the fluid the melting temperature rises as the concentration of $H_2O$ in the silicate liquid phase decreases. Estimates for the $H_2O$ content of the silicate liquid are shown in values of weight percent along the melting curve (Holloway 1973).

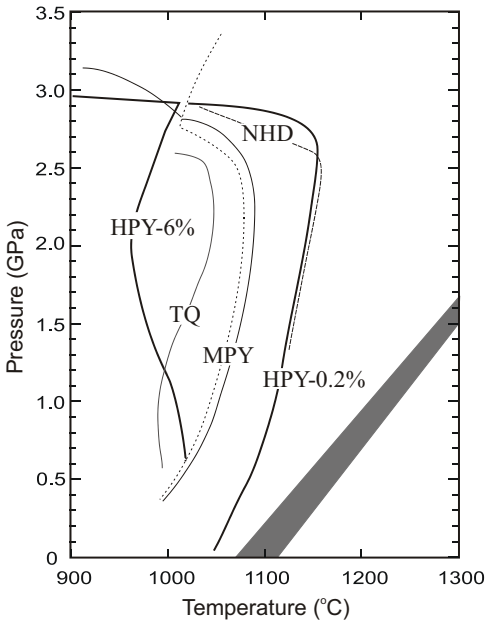


**Figure 5.** Pargasite amphibole stability curves in peridotite bulk compositions at water saturated and under-saturated conditions. HPY-6% denotes the limit of pargasite stability in a Hawaiian pyrolite composition at $H_2O$ saturated conditions with 6 wt% $H_2O$ (Green 1973). HPY-0.2% is the same peridotite composition at under-saturated conditions with 0.2 wt% $H_2O$. NHD is North Hessian Depression peridotite at $H_2O$ undersaturated conditions with 0.15% $H_2O$ (Mengel and Green 1989). TQ is $H_2O$ undersaturated Tinaquillo lherzolite with 0.2% $H_2O$ (Wallace and Green 1991). MPY is $H_2O$ undersaturated MORB pyrolite with 0.6% $H_2O$ (Niida and Green 1999). For the MPY (MORB pyrolite) composition the vapor absent solidus is also indicated a few degrees below the amphibole breakdown curve by a dashed curve. The dry solidi for these peridotite compositions occur in the grey region.

conditions (HPY-6%). Under both $H_2O$-saturated and -undersaturated conditions the studies are consistent with amphibole disappearing from the assemblage a few degrees above the solidus. The fluid-absent solidus, indicated as the dashed line for MORB pyrolite (MPY), is in fact controlled by the amphibole stability field and backbends sharply as amphibole becomes unstable. It should be noted, however, that Mysen and Boettcher (1975) studied 4 peridotite compositions at water-saturated conditions and found significantly lower solidus temperatures and lower amphibole thermal stability limits than those reported by Green (1973). Kushiro (1970) and Millhollen et al. (1974), however, reported similar phase relations to those of Green (1973). Possible causes for these differences are discussed by Gilbert et al. (1982; page 299).

The variable extent of the amphibole stability field under fluid absent conditions (variations by about 0.5 GPa and more than 100 °C) has been attributed to variations in alkali and Ti contents of the bulk compositions (Niida and Green 1999). The bulk composition with the lowest alkali content shows the smallest amphibole stability field (Tinaquillo lherzolite;

Wallace and Green 1991) whereas the highest alkali content results in the largest stability field (Hawaiian pyrolite; Green 1973). This is somewhat counter intuitive as it means the less fertile, alkali poor samples melt at a lower temperature. Wallace and Green (1991), however, rationalized this in terms of the alkali/$H_2O$ ratio. If the alkali/$H_2O$ ratio of the bulk composition is low then the proportion of amphibole formed at high temperatures will not be sufficient to account for the entire $H_2O$ content. The excess $H_2O$ will induce melting, which will strongly partition alkalis to the melt and lead to amphibole breakdown. Figure 6 shows how pargasite alkali contents increase in both *A* and *B* sites with increasing pressure. The data cover temperatures between 925-1150 °C and there is also an increase in amphibole alkali contents over this temperature range. In addition to pargasite, the Na content of coexisting clinopyroxene also increases with pressure. As there is no other alkali-bearing phase a decrease in the modal abundance of pargasite must also occur with increasing *P* and *T*. It is most likely this relationship that ultimately leads to an excess of $H_2O$ over alkalis and melting.

## Apatite

Relatively little experimental work exists on the stability of apatite $Ca_5(PO_4)_3(OH,F,Cl)$ particularly in natural rock systems at high pressures. The melting curves of pure hydroxyl $Ca_5(PO_4)_3(OH)$ and fluor $Ca_5(PO_4)_3(F)$ apatites were approximately determined by Murayama et al. (1986) with the melting temperature of hydroxyl apatite rising from 1613 °C at atmospheric pressure to over 2000 °C at 7.7 GPa. Melting temperatures of fluor apatite are slightly higher. Above 10 GPa both end-members breakdown to gamma-$Ca_3(PO_4)_2$ plus either CaF or CaO + $H_2O$. Several studies have examined the solubility of apatite in a variety of melt compositions at high pressures. Watson (1980) observed that the high solubility of apatite in basic silicate melt compositions meant that it was unlikely to remain as a residual phase in the mantle during significant partial melting and may not, therefore, influence the trace element

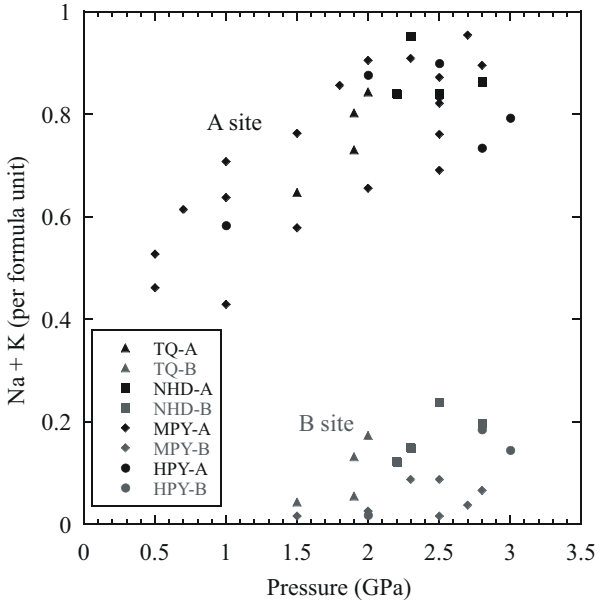


**Figure 6.** Pressure variation of the total alkali content (Na+K) in the *A* site and Na content in the *B* site of pargasitic amphibole (general formula $A_{0-1}B_2C_5T_8O_{22}(OH)_2$) from the water-under saturated experimental studies of Green (1973), Mengel and Green (1989), Wallace and Green (1991) and Niida and Green (1999). Peridoitie composition abbreviations are the same as in Figure 5.

composition of melts. Watson (1980) reasoned, however, that it might remain as a residual phase during melting at lower temperatures in the presence of $H_2O$. Baker and Wyllie (1992) measured apatite solubility in equilibrium with low degree $H_2O$ bearing carbonatite melts in equilibrium with mantle peridotite and found apatite to melt out close to the solidus. For fluid undersaturated conditions compatible with rocks containing only apatite, the thermal stability of apatite may be quite high, but the onset of melting due to the presence of other hydrous phases such a pargasite may strongly reduce apatite thermal stability.

**Phlogopite**

Studies by Sato et al. (1997) and Trønnes (2002) on the stability field of phlogopite at high pressure report very similar decomposition curves (Fig. 7). Trønnes (2002) found that synthetic end member phlogopite in the KMASH system undergoes dehydration melting to an assemblage of pyrope, forsterite and liquid up to ca. 8 GPa and an assemblage of pyrope, Phase X, forsterite and liquid above 9 GPa. Sato et al. (1997) used a natural phlogopite composition that was Al-rich (ca. 10% eastonite component) and found an incipient breakdown at high pressure to produce phlogopite, closer to the end member composition, and garnet and fluid.

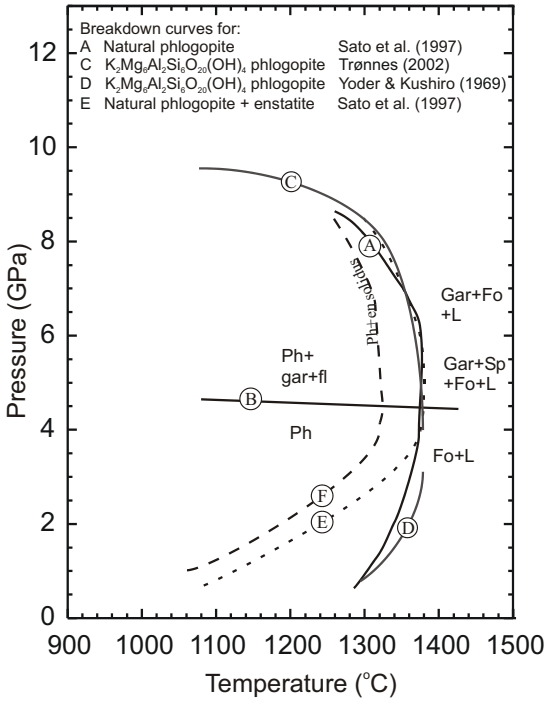


**Figure 7.** The stability of phlogopite and phlogopite plus enstatite from various experimental studies. (A) The stability field of a natural phlogopite $K_{2.1}Na_{0.1}Mg_{5.4}Fe_{0.2}Al_{2.5}Si_{5.7}O_{20}(OH,F)_4$ (Sato et al. 1997) with the breakdown products at various pressures indicated on the diagram. Above the curve (B) excess Al in the natural phlogopite is expelled and produces garnet and fluid. The curves labeled (C) and (D) show the breakdown of synthetic $K_2Mg_6[Si_6Al_2]O_{20}(OH)_4$ phlogopite from Trønnes (2002) and Yoder and Kushiro (1969), respectively. The breakdown products are similar to those found by Sato et al, (1997) except that curve (B) was not observed and above 9 GPa the products were pyrope, Phase X, forsterite and liquid. (E) shows the breakdown curve of a natural phlogopite plus enstatite assemblage determined by Sato et al. (1997) which occurs above the solidus indicated by curve (F). Data of Modreski and Boettcher (1972) constrain both (E) and (F) at pressures below 4 GPa.

The onset of this breakdown is indicated by curve (F) in Figure 7. These results imply that the $AlAlMg_{-1}Si_{-1}$ eastonite substitution becomes unstable at high pressures. The similar thermal stability range of the ideal phlogopite end member (Yoder and Kushiro 1969; Trønnes 2002) and the natural Al-rich phlogopite (Sato 1997) may be coincidental. The natural phlogopite also contained significant amounts of F and Fe, which could have stabilizing and destabilizing effects, respectively.

Sato et al. (1997) also studied the stability of the same natural phlogopite composition coexisting with enstatite. They observed the same shift in phlogopite composition with pressure and a similar stability field for phlogopite above 4 GPa. The solidus, however, is displaced to lower temperatures by approximately 50  with phlogopite coexisting with melt over this temperature interval. Below 4 GPa the stability field of phlogopite and enstatite becomes significantly smaller than that of pure phlogopite as shown by the data of Modreski and Boettcher (1972).

Two studies have examined the stability of phlogopite plus diopside assemblages in the KCMASH system (Sudo and Tatsumi 1990; Luth 1997) as shown in Figure 8. In a Ca bearing system K-richterite amphibole is stable and becomes a high-pressure product of phlogopite decomposition. Sudo and Tatsumi (1990) proposed that in idealized terms this reaction is

$$\underset{\textit{phlogopite}}{2K_2Mg_6Al_2Si_6O_{20}(OH)_4} + \underset{\textit{diopside}}{2CaMgSi_2O_6} =$$

$$\underset{\textit{KK-richterite}}{K_2CaMg_5Si_8O_{22}(OH)_2} + \underset{\textit{garnet}}{CaMg_5Al_4Si_6O_{24}} + \underset{\textit{forsterite}}{2Mg_2SiO_4} + [\underset{\textit{fluid}}{K_2O+3H_2O}] \qquad (5)$$

In the Na-free system, K occupies both *A* and *B*(M4) sites in amphibole and is referred to a KK-richterite, as opposed to ordinary mantle K-richterites which are closer to the general formula $KNaCaMg_5Si_8O_{22}(OH)_2$. Sudo and Tatsumi (1990) showed that reaction (5) was divarient and occurred over a pressure interval of approximately 5 GPa. The results of Luth (1997) combined with those of Sudo and Tastumi (1990) indicate that phlogopite starts to

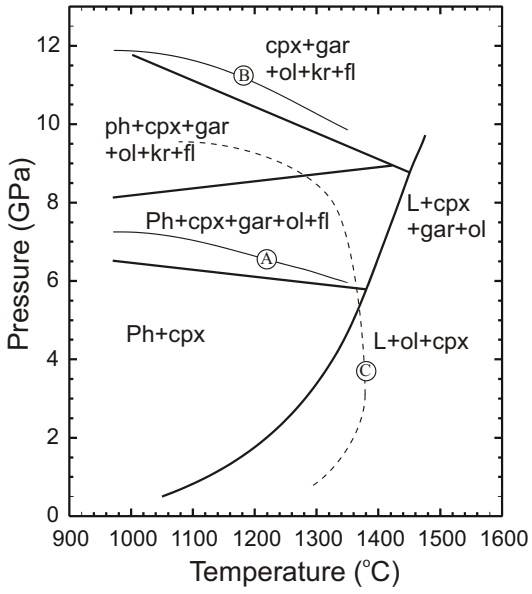


**Figure 8.** The stability of phlogopite coexisting with diopside in the KCMASH system from Luth (1997). All labeled fields and solid thick curves refer to those reported by Luth (1997). Curves (A) and (B) are those reported by Sudo and Tatsumi (1990). Curve (C) shows the stability of pure phlogopite from Trønnes (2002) and Yoder and Kushiro (1969).

breakdown to produce garnet at pressures lower than where K-richterite is observed in the experimental charges. This results in a field of phlogopite+ diopside + garnet, which must also coexist with fluid. Luth (1997) bracketed the high temperature breakdown of phlogopite, by melting of the diopside + phlogopite + garnet assemblage, at between 1400 and 1450 °C at 7.5 GPa. This is one of the highest temperature occurrences reported for phlogopite in ultramafic systems and is difficult to reconcile with the lower thermal stability of pure phlogopite.

Konzett and Ulmer (1999) studied the stability of K-bearing phases at high pressure and temperature in an analogue KNCMASH lherzolite-30% olivine composition and in a natural lherzolite composition. As shown in Figure 9 in the KNCMASH system, the maximum pressure and temperature stability of phlogopite is much smaller than that reported by Luth (1997). The lower pressure stability of phlogopite in the bulk composition studied is explained by the presence of enstatite, which instigates phlogopite breakdown via the reaction,

$$\underset{\textit{phlogopite}}{2K_2Mg_6Al_2Si_6O_{20}(OH)_4} + \underset{\textit{diopside}}{CaMgSi_2O_6} + \underset{\textit{enstatite}}{Mg_2Si_2O_6} =$$

$$\underset{\textit{KK-richterite}}{K_2CaMg_5Si_8O_{22}(OH)_2} + \underset{\textit{garnet}}{2Mg_3Al_2Si_3O_{12}} + \underset{\textit{forsterite}}{2Mg_2SiO_4} + [\underset{\textit{fluid}}{K_2O + 3H_2O}] \qquad (6)$$

as initially proposed by Sudo and Tatsumi (1990) for a Na-free system. In the bulk composition studied by Konzett and Ulmer (1999) phlogopite persisted to higher pressure as a result of enstatite being exhausted by reaction (6), whereas in natural compositions, where the modal abundance of phlogopite is likely less than enstatite, this would not occur. In the natural lherzolite composition studied by Konzett and Ulmer (1999) reaction (6) is displaced to lower pressure by approximately 1 GPa, most likely as a result of Fe which partitions more favorably into garnet on the right side of Equation (6). At lower pressure the stability of phlogopite in a natural lherzolite composition minus 60% olivine and with 0.4% $K_2O$ and $H_2O$ was studied by Mengel and Green (1989). Phlogopite was observed to persist above the solidus, which below 2.5 GPa appears to be coincident with the melting out of pargasitic amphibole.

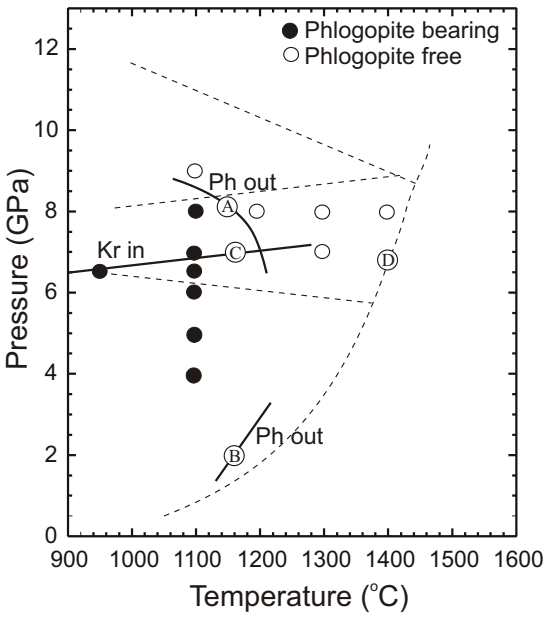


**Figure 9.** The stability of phlogopite in a synthetic KNCMASH lherzolite-30% olivine composition Konzett and Ulmer (1999). Closed and open symbols bracketing curve (A) indicate assemblages where phlogopite was present and absent, respectively. Olivine, garnet and clinopyroxene are present at all conditions. Orthopyroxene is present at pressures below curve (C), which is Equation (7) given in the text, above which K-richterite becomes stable. The temperature stability of phlogopite determined by Mengel and Green (1989) in a North Hessian Depression peridotite composition is shown by curve (B) whereas the phase relations of Luth (1997) for phlogopite plus diopside are shown by the dashed curve labeled (D).

As shown in Figure 10 experimental studies show that phlogopite alumina contents in peridotite bulk compositions decrease with pressure (Konzett and Ulmer 1999; Mengel and Green 1989). This is in good agreement with natural phlogopite occurrences from lower pressure spinel and higher pressure garnet peridotites (Fig. 2a). In addition, the data at 6.5 GPa, covering an experimental temperature range from 850 to 1100 °C, show a small increase of Al content with increasing temperature.

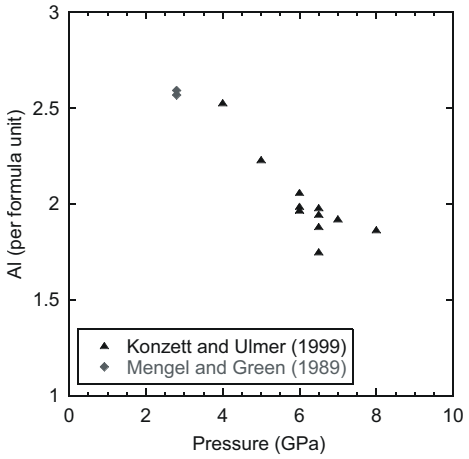


**Figure 10.** Phlogopite Al content in atoms per formula unit versus pressure for experimental samples produced within peridotite bulk compositions by Konzett and Ulmer (1999) and Mengel and Green (1989) between 850 and 1195 °C.

## K-richterite

Hübner and Papike (1970) first synthesized K-richterite ($KNaCaMg_5Si_8O_{22}(OH)_2$) and recognized its potential high pressure stability as it has a smaller molar volume than the corresponding product assemblage phlogopite and diopside. The high pressure stability field of the pure $KNaCaMg_5Si_8O_{22}(OH)_2$ phase, as bracketed by Trønnes (2002), extends to pressures slightly greater than 14 GPa (Fig. 11). The maximum thermal stability is approximately 1450 °C and occurs at 10 GPa. The Na-free KK-richterite ($K_2CaMg_5Si_8O_{22}(OH)_2$) has a stability field that extends to higher pressure by approximately 1 GPa, as determined by Inoue et al. (1998).

K-richterite could form in the mantle in two quite different bulk compositions. The first, which accounts for virtually all natural xenolith samples, is in garnet-free peralkaline ultrabasic rocks such as the MARID suite and the strongly metasomatized peridotites termed PKP where $(Na_2O+K_2O)/Al_2O_3 > 1$. The second is not naturally observed but would be normal subalkaline lherzolite rocks at pressures above 6-7 GPa, as discussed later. Konzett et al. (1997) and Konzett and Fei (2000) have shown that the K/Na ratio of K-richterite increases with pressure in both peralkaline and subalkaline bulk compositions. The K/Na ratio of experimentally produced K-richterite reflects the K/Na ratio of the bulk composition, which, as Konzett et al. (1997) point out, is quite different to natural MARID rocks. K-richterites in MARIDs have a generally narrow range of K/Na ratio even though the bulk rocks have a far more variable range. As Konzett et al. (1997) reasoned, this means that MARID rocks themselves cannot represent the entire liquid from which the rocks crystallized, i.e., MARID rocks are cumulates.

The results of Konzett et al. (1997) and Konzett and Fei (2000) demonstrate that in peralkaline bulk compositions, where diopside is stable but garnet is only present at pressures >8 GPa, K-richterite stability is very close to that of the pure phase. Only the thermal maxima is reduced by approximately 100 °C compared to the pure phase stability determined by Trønnes (2002). The vast majority of mantle peridotite rocks, on the other hand, are subalkaline (i.e., $Na_2O+K_2O)/Al_2O_3 > 1$). K-richterite is only stable in subalkaline lherzolitic bulk compositions above 6-7 GPa as a result of the reaction:

$$\underset{\textit{phlogopite}}{0.5K_2Mg_6Al_2Si_6O_{20}(OH)_4} + \underset{\textit{in cpx}}{CaMgSi_2O_6} + \underset{\textit{opx}}{NaAlSi_2O_6 + Mg_2Si_2O_6} =$$

$$\underset{\textit{K-richterite}}{KNaCaMg_5Si_8O_{22}(OH)_2} + \underset{\textit{garnet}}{Mg_3Al_2Si_3O_{12}} \qquad (7)$$

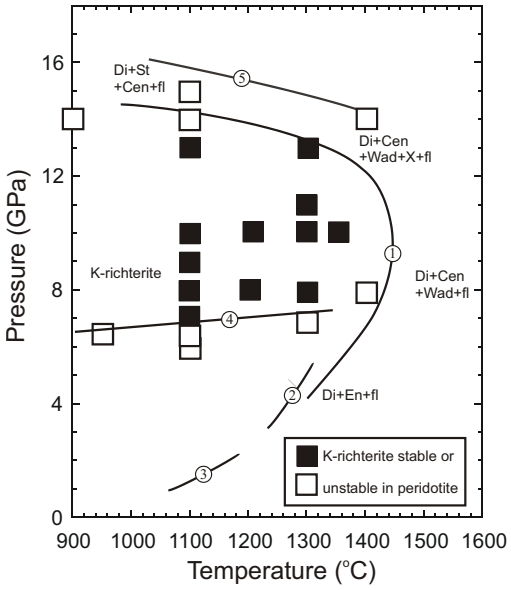


**Figure 11.** The stability field of pure $KNaCaMg_5Si_8O_{22}(OH)_2$ K-richterite as bracketed by Trønnes (2002) is shown by curve (A). All of the indicated named products are with respect to curve (A) with Wad being wadite-structured $K_2Si_4O_9$, X is Phase X, en and Cen are enstatite and clinoenstatite, Di is diopside and St is stishovite. Curves (B) and (C) are stability fields of K-richterite determined by Foley (1991) and Gilbert and Briggs (1974), respectively. The closed and open symbols indicate the presence and absence of K-richterite in a synthetic KNCMASH subalkaline peridotite assemblage, as determined by Konzett and Ulmer (1999) and Konzett and Fei (2000). In these experiments the coexisting assemblage always contained olivine, garnet, clinopyroxene and enstatite or clinoenstatite. The breakdown products at high pressure also contain Phase X and below curve (D) K-richterite breaks down to a phlogopite-bearing assemblage. Curve (E) shows the high pressure stability of KK-richterite $K_2CaMg_5Si_8O_{22}(OH)_2$ as determined by Inoue et al. (1998).

Equation (7), the Na present equivalent of Equation (6) proposed by Sudo and Tatsumi (1990), demonstrates that the breakdown of minor amounts of phlogopite in the presence of pyroxenes containing some jadeite component can produce the observed natural mantle K-richterite without any fluid release. The identical K/OH-ratio of phlogopite and K-richterite (but not KK-richterite) is the fundamental requirement for such a fluid-free reaction (Konzett and Ulmer 1999). Equation (7) and the general lack of K-richterite in garnet-bearing mantle xenoliths (e.g., Erlank et al. 1987), indicate that the majority of such xenoliths equilibrated at depths shallower than 200 km.

## EXPERIMENTAL STUDIES ON THE STABILITY OF POTENTIAL HIGH PRESSURE HYDROUS MANTLE MINERALS

Whereas most mantle xenoliths originate from the upper 200 km of the mantle or up to approximately 7 GPa, experimental studies at higher pressures have identified a number of other hydrous minerals that are potentially stable in the deeper parts of the mantle, although mainly in subduction zones. These phases generally don't have mineral names and are simply referred to by letters e.g., A, B, superhydrous B, D, E and X. Their stability in subduction zones is covered in this volume by Kawamoto (2006). The criterion for evaluating their presence in the ambient mantle is their compatibility with typical mantle minerals and their high temperature stability,

which can only be assessed through experimental studies. Here I only consider phases with upper thermal stability limits that are close to an average mantle adiabat.

**Phase X**

The enigmatically named Phase X has been observed in several studies as a high-pressure product of the decomposition of K-richterite. Phase X has a variable composition with reported $K_2O$ contents of between 10 and 19 wt%. In the KCMSH system Inoue et al. (1998) reported Phase X with the approximate composition $K_4Mg_8Si_8O_{25}(OH)_2$ whereas Trønnes (2002) reported the composition $K_{3.7}Mg_{7.4}Al_{0.6}Si_8O_{25}(OH)_2$ in the KMASH system. In addition to Phase X with the formula $K_{1.54}Mg_{1.93}Si_{1.89}O_7H_{1.04}$, Yang et al. (2001) synthesized and solved the structures of sodic Phase X, $Na_{1.16}K_{0.01}Mg_{1.93}Al_{0.14}Si_{1.89}O_7H_{1.04}$, and the anhydrous end members $K_{1.85}Mg_{2.06}Si_{2.01}O_7$ and $Na_{1.78}Mg_{1.93}Al_{0.13}Si_{2.02}O_7$. Phase X is composed of layers of brucite-like $MgO_6$ octahedra linked by $Si_2O_7$ tetrahedral dimers and K cations (Yang et al. 2001; Mancini et al. 2002). Yang et al. (2001) proposed the general formula $A_{2-x}M_2Si_2O_7H_x$ where $A$ can be K and/or Na, $M$ can be Mg or Al and $x$ = 0-1. An increase in the K content of Phase X is therefore coupled to a decrease in the H content. The only measurement of the $H_2O$ content of Phase X, performed using SIMS, yielded a value of 1.7±0.1 wt% $H_2O$ (Inoue et al. 1998), which is significantly below the theoretical maximum of 3.51 wt%.

No studies have been performed on the stability of any pure Phase X composition; however, Konzett and Fei (2000) have examined the stability of Phase X in a subalkaline KNCMASH analogue peridotite composition. Phase X coexists with a typical mantle assemblage of olivine/wadsleyite, clinopyroxene and garnet between 14 and 20 GPa and at temperatures up to 1600 °C. Phase X, therefore, has the highest thermal stability of any yet investigated nominally hydrous silicate. As shown in Figure 12 the high temperature stability of Phase X is for the main part undetermined. Konzett and Fei (2000) showed that the reactions that produce Phase X from K-richterite in a mantle peridotite composition release fluid because the K/H ratio of Phase X is higher than that of K-richterite. These results also show that the K content and K/Na ratio of Phase X both increase with pressure, which implies a decrease in the $H_2O$ content of Phase X with pressure. The change in K/Na ratio occurs as Na is partitioned into coexisting garnet with increasing pressure. Between 20 and 22 GPa Phase X breaks down to an assemblage containing K-hollandite ($KAlSi_3O_8$).

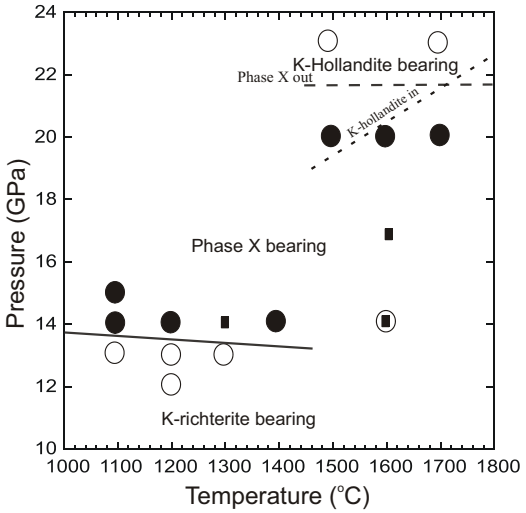


**Figure 12.** The closed and open symbols indicate the presence and absence of phase-X in a synthetic KNCMASH subalkaline peridotite assemblage, as determined Konzett and Fei (2000). In these experiments the coexisting assemblage was that expected for a peridotite composition at the indicated conditions, i.e., olivine or high-pressure polymorphs, garnet and Ca-perovskite at and above 20 GPa. Filled rectangles show conditions where Luth (1997) observed Phase X in a KCMASH bulk composition. At high pressures Phase X breaksdown to an assemblage containing K-hollandite ($KAlSi_3O_8$).

**Humite and dense hydrous magnesium silicate phases**

A number of high pressure experimental studies have shown that the humite minerals chondrodite and clinohumite and the dense hydrous magnesium silicate phases A, superhydrous B, D and E can coexist with ultramafic assemblages at various conditions above 6 GPa and below 1200 °C (Kanzaki 1991; Kawamoto et al. 1995; Ohtani et al. 1995; Frost and Fei 1998; Irifune et al. 1998). The stability fields of these phases are significantly below reasonable average mantle adiabats and they are therefore only expected to be stable in the cooler regions of subduction zones, provided that significant $H_2O$ is in fact present within such regions at pressures above 6 GPa. Although the stability fields have been examined in natural systems (Luth 1995; Kawamoto et al. 1995; Frost 1999; Kawamoto 2004) there remains some question as to whether the strong partitioning of some element by a particular hydrous phase may cause some increase in thermal stability. In addition the large amounts of $H_2O$ added in some bulk compositions may result in the breakdown of hydrous phases at a lower temperature than we might expect in the mantle as a result of excessive melting. Experiments in relatively low-$H_2O$ bulk compositions show, however, that the presence of Al and Fe in phases A and E, superhydrous phases B and D has a limited effect on stability relations in comparison to the MSH system (Luth 1995; Frost 1999). Humite minerals have a preference for Ti and F. Titanian clinohumite is a common accessory mineral in metamorphosed ultrabasic rocks and occurs in serpentinites and kimberlites (López Sánchez-Vizcaíno et al. 2005). The stability of titanian clinohumite is below 1000 °C at 8 GPa although the pure fluorine clinohumite end-member is stable to over 1400 °C at 3 GPa (Weiss 1997; Ulmer and Trommsdorf 1999). The experiments of Kawamoto (2004) contained Ti and showed clinohumite and chondrodite stability to be limited to below 1100 °C at 11 GPa.

Phase D is the highest-pressure dense hydrous magnesium silicate and its stability in the lower mantle is ultimately controlled by the reaction,

$$\underset{\textit{Phase D}}{MgSi_2O_4(OH)_2} + \underset{\textit{periclase}}{MgO} = \underset{\textit{MgSi-perovskite}}{2MgSiO_3} + \underset{\textit{Liquid}}{H_2O} \quad (8)$$

The slope of this reaction is not clear however. From a Schreinemakers analysis of the existing experimental data Komabayashi et al. (2004) reported a negative Clapyron slope at approximately 25 GPa with a maximum thermal stability for phase D of 1100°C. Laser heated diamond cell experiments of Shieh et al. (1998) indicate that this reaction leads to the breakdown of phase D at 44 GPa at temperatures between 1000 and 1400 °C, which would be consistent with a convex shape of the reaction boundary of Equation (8), like many other dehydration reactions. Phase D may therefore be stable at temperatures higher than 1100 C at pressures between 25 and 44 GPa but it is probably unlikely that these temperatures approach that of the mantle adiabat. In natural systems phase D contains significant amounts of Al and ferric and ferrous Fe but not in quantities higher than coexisting silicate perovskite, so they have little effect on the thermal stability of phase D (Frost 1999; Frost unpublished data).

## THE STABILITY OF HYDROUS PHASES IN ULTRAMAFIC LITHOSPHERE AND THE CONVECTING MANTLE

In considering the significance of hydrous minerals in the mantle it is not only of interest to define stability fields, but it is also important to assess the proportion of hydrous minerals that may exist at particular conditions, identify how much of the mantle's water budget they may account for and examine further factors, such as $H_2O$ activity, that may affect their stability. Changing redox conditions as a function of depth in the upper mantle and transition zone may also control fluid speciation and $H_2O$ activity, which, in turn, may affect the stability of the hydrous phases.

Figure 13 shows the stability fields of the major mantle hydrous phases derived from the previously described experimental studies. The experimental data employed are from studies where hydrous phases formed in equilibrium with typical ultramafic mantle assemblages at $H_2O$ undersaturated conditions. A mantle adiabat with a potential temperature of 1600 K (i.e., the temperature at the surface when extrapolated through the melting region) is shown with branching geotherms for Achean cratonic and oceanic lithosphere. A water saturated peridotite solidus interpolated from the data of Mysen and Boettcher (1975) to 4 GPa and Kamamoto (2004) >4 GPa is shown. The solidus is not followed into the region of dense hydrous magnesium silicate stability because huge amounts of $H_2O$ are required to produce a melt at these conditions and the solvus between fluid and melt may anyway disappear.

Figure 13 indicates that the only hydrous mineral to be stable along an average mantle adiabat (AMA) is Phase X, which could be present in the mantle between depths of 400 and 600 km. The Archean lithospheric geotherm (ACL), which branches off the average mantle adiabat at temperatures approaching 1400 °C, misses the stability field of K-richterite but enters the phlogopite stability field at pressures of approximately 6.8 GPa at 1280 °C. In Figure 13 the data on phlogopite and K-richterite are taken from experiments in Fe-free systems (Konzett and Ulmer 1999; Konzett and Fei 2000). Preliminary experiments seem to indicate that Fe destabilizes these hydrous phases further (Konzett and Ulmer 1999) and the extent of the stability fields in Figure 13 may, therefore, be slightly overestimated. It is important to reiterate that in nature K-richterite occurs in mantle xenoliths of peralkline rocks where the K-richterite stability field extends to much lower pressures (Konzett et al. 1997) than in normal subalkaline

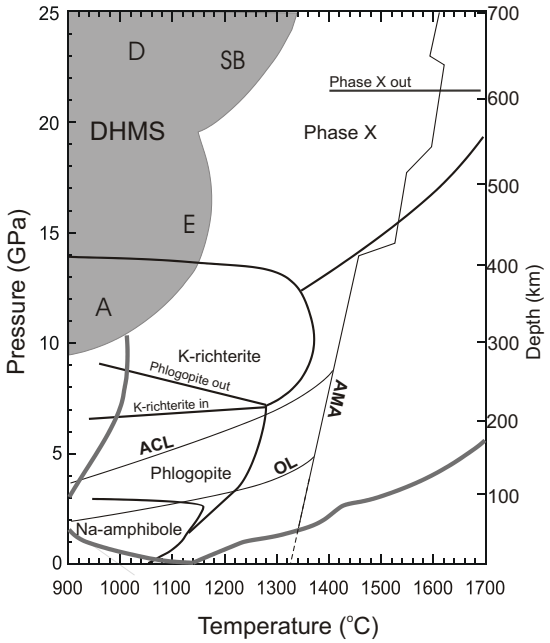


**Figure 13.** Stability fields of hydrous minerals in mantle of peridotite composition at $H_2O$-undersaturated conditions. Data are combined from Figures 5,9,11 and 12. The grey shaded region shows where the dense hydrous magnesium silicate phases A, E, super hydrous phase B (sB) and D are stable from Kawamoto (2005). Thick grey curves show the peridotite solidus under $H_2O$ saturated and dry conditions. An average mantle adiabat (AMA) and geotherms for Archean cratonic lithosphere (ACL) and 100 million year old oceanic lithosphere (OL) are shown by thin black lines.

peridotite compositions that are depicted in Figure 13. It seems that the only environment where K-richterite could exist in subalkaline mantle rocks is in a subduction zone. The oceanic lithosphere geotherm (OL) passes into the stability field of phlogopite and pargasitic amphibole below 3 GPa.

The proportion of hydrous minerals that form along typical geotherms will depend on the Na and K content of the mantle, which in turn will depend on the degree of depletion and metasomatism. Using a primitive mantle composition as a benchmark, it is possible to appreciate the degree of metasomatic enrichment necessary for significant hydrous minerals to form in the lithosphere. If we consider a typical primitive mantle $Na_2O$ content of 0.3 wt% then from the experiments of Niida and Green (1999) we can calculate that along an oceanic geotherm at approximately 70 km the lherzolitic assemblage could contain 9 wt% pargasitic amphibole which would accommodate approximately 1500 ppm $H_2O$, assuming stoichiometric amphibole OH contents. At only 50 km this rises to approximately 25 wt% pargasite which would host 4000 ppm $H_2O$ in the bulk. Significant amounts of amphibole can, therefore, form in lithospheric mantle with typical Na contents, mostly at the expense of clinopyroxene, by adding relatively small amounts of $H_2O$ alone. Primitive mantle K contents, on the other hand, are generally 10 times lower than corresponding Na contents. Therefore, along an Archean craton lithospheric geotherm at approximately 150 km depth 0.03 wt% $K_2O$ in the bulk rock will allow a maximum of just 0.2 wt% phlogopite to form, which will host 90 ppm $H_2O$, using data from Konzett and Ulmer (1999). In comparison, metasomatized garnet phlogopite peridotite rocks (GPP) reported by Erlank et al. (1987) have average bulk $K_2O$ contents of 0.16% which would result in 1.4 wt% phlogopite forming at 150 km with a bulk $H_2O$ content of 600 ppm. Erlank et al. (1987) classified GPP rocks as the least metasomatized, whereas PKP rocks, which are considered to be the most metasomatized, have average $K_2O$ contents of approximately 1%. The presence of significant phlogopite in some mantle xenoliths means, therefore, that there are processes that occur in the mantle that strongly concentrate K while having much smaller effects on other major elements and in particular Na. One possibility is that such high K-bearing liquids are produced by the breakdown of the white mica phengite in subducting lithosphere (Schmidt et al. 2004). If this is the only explanation then all K-rich metasomatism of the lithosphere must be related to subduction. Another possibility is that high-pressure metasomatic fluids or melts are K-rich because Na becomes compatible in clinopyroxene during melting at high pressures and low temperatures (Blundy et al. 1995). Clinopyroxene/melt partition coefficients for K, on the other hand, are normally 2 orders of magnitude below those of Na. The compositions of low-fraction hydrous melts or fluids at pressures above 3 GPa are poorly constrained but further study may provide important insights into metasomatic agents in the lithosphere.

Phase X is the only hydrous mineral that could be stable along an average mantle adiabat in the convecting mantle, at least given the available experimental data that extend to lower mantle conditions (>660 km). Assuming a primitive mantle bulk composition we can calculate how much Phase X could form at the top of the transition zone (410 km) and how much of the convecting mantle's water budget it could account for at these depths. Using the data of Konzett and Fei (2000) who used a $K_2O$ enriched KLB-1 peridotite composition the $K_2O$ content of Phase X expected in the transition zone is 14.5 wt% and the stoichiometric $H_2O$ content is approximately 3 wt%. If the bulk rock contains 0.03 wt% $K_2O$ then 0.1 wt% Phase X can form with the proportion of $H_2O$ hosted by Phase X being just 30 ppm. In addition to the low K content of the primitive mantle, at these conditions high Ca-clinopyroxene also contains as much as 0.1% $K_2O$ and given the uncertainty on some of the values it is quite possible that all $K_2O$ and $H_2O$ may be accommodated by the nominally anhydrous assemblage. It is of course also possible that K is inhomogeneously distributed in the convecting mantle in a similar way to that found in the lithosphere, resulting in regions with higher proportions of Phase X. If the bulk of the transition zone has a primitive mantle composition, however, then the formation of these regions must leave the remaining transition zone depleted in K and the amount of $H_2O$ stored

by Phase X over the bulk of the transition zone cannot be much greater than 30 ppm. It seems clear, therefore, that nominally anhydrous minerals and melts, or possibly fluids at reducing conditions, must host the majority of hydrogen stored in the ambient convecting mantle.

As shown in Figure 4 and explained previously for pargasitic amphibole, hydrous phases display the highest thermal stability at fluid-absent conditions. Figure 13 should, therefore, depict the maximum thermal stability within ultramafic bulk compositions with respect to water activity. Lower $H_2O$ activities or $H_2O$-saturated conditions should lead to lower hydrous mineral stability fields. One of the problems of relating experimental studies of hydrous mineral stability to natural mantle mineral assemblages is that we generally have only circumstantial evidence for the nature of the metasomatic or igneous melt/fluid phase from which the minerals formed. The activity of $H_2O$ at the conditions of formation are, therefore, poorly constrained. For this reason the previously described methodology of Popp et al. (1995) to determine $H_2O$ activity through the use of Equation (2) is particularly attractive. Above subduction zones for example where high concentrations of $H_2O$ may enter the mantle wedge the maximum thermal stability of hydrous minerals such as pargasite or phlogopite may be closer to that of $H_2O$-saturated conditions, shown for pargasite in Figures 4 and 5, which may be a few hundred degrees below those in Figure 13.

Another poorly constrained factor is that the oxygen fugacity of the mantle may decrease with depth causing C-O-H fluids to become richer in $CH_4$ and lowering the activity of $H_2O$ (Woermann and Rosenhauer 1985; Wood et al. 1990). Several studies have argued for a lowering of mantle $fo_2$ with depth as a result of the pressure effect on the ferric-ferrous equilibria that likely define mantle $fo_2$ and due to changes in the solubility of ferric iron in major mantle minerals (Wood et al. 1990; Gudmundsson and Wood 1995; O'Neill et al. 1993; Ballhaus and Frost 1994; Frost et al. 2004). Several oxygen thermobarometry studies on garnet peridotite xenoliths have observed a decrease in $fo_2$ with depth from values of around FMQ-1 (one log unit below the fayalite-magnetite-quartz oxygen buffer) close to the spinel peridotite field at 80 km depth down to FMQ-4 at approximately 200 km (McCammon et al. 2001; Woodland and Koch 2003; McCammon and Kopylova 2004). O'Neill et al. (1993) argued that oxygen fugacities in the transition zone may be close to the iron-wüstite buffer (IW i.e., ~FMQ-5). At these conditions a C-O-H fluid may contain over 50% $CH_4$ and up to 5% $H_2$ although values are uncertain as equations of states for reduced gas phases are poorly constrained at these conditions (Holloway 1987; Belonoshko and Saxena 1992). $H_2$ contents may also increase depending on the activity of carbon and components such as $H_2S$ could also be relevant. Although there is very little experimental data on their behavior, reduced fluid phases may be more mobile in the mantle as their components likely have lower solubilities in minerals and melts and the solubilities of silicate components in these fluids may be low. As previously discussed, Taylor and Green (1988) observed an increase in the fluid-saturated peridotite solidus between 1.0 and 3.5 GPa at low $fo_2$ (~FMQ-4) where $CH_4$ became a major fluid component. This occurred because $CH_4$ lowered the $H_2O$ activity in the fluid, which lowered the $H_2O$ solubility in the coexisting silicate melt. The presence of a reduced fluid phase with a low $H_2O$ activity in the mantle may affect hydrous phase stability and may also lower the solubility of hydroxyl in nominally anhydrous phases. The mobility and low density of a reduced fluid phase in the deeper convecting mantle may help to redistribute hydrogen and might even tend to focus $H_2O$ in the upper more oxidized regions of the upper mantle.

## ACKNOWLEDGMENTS

I am tremendously grateful to Jurgen Konzett, Reidar Trønnes and Alan Woodland for lengthy discussions and for making numerous comments on an earlier version of the manuscript. I also appreciate the comments and corrections of Hans Keppler and John Winter.

## REFERENCES


Adam J, Green TH, Sie SH (1993) Proton microprobe determined partitioning of Rb, Sr, Ba, Y, Nb and Ta between experimentally produced amphiboles and silicate melts with variable F content. Chem Geol 109: 29-49

Adam J, Green TH, Sie SH, Ryan CG (1997) Trace element partitioning between aqueous fluids, silicate melts and minerals. Eur J Mineral 9:569-584

Arai S, Matsukage K, Isobe E, Vysotskiy S (1997) Concentration of incompatible elements in oceanic mantle: effect of melt/wall interaction in stagnant or failed melt conduits within peridotite. Geochim Cosmochim Acta 61:671-675

Agrinier P, Mevel C, Bosch D, Javoy M (1993) Metasomatic hydrous fluids in amphibole peridotites from Zabargad island (Red Sea). Earth Planet Sci Lett 120:187-205

Baker MB, Wyllie PJ (1992) High-pressure apatite solubility in carbonate-rich liquids: implications for mantle metasomatism. Geochim Cosmochim Acta 56:3409-3422

Bailey DK (1982) Mantle metasomatism-continuing chemical change within the Earth. Nature 296:525-530

Ballhaus C, Frost BR (1994) The generation of oxidized $CO_2$-bearing basaltic melts from reduced $CH_4$-bearing upper mantle sources. Geochim Cosmochim Acta 58:4931-4940

Belonoshko AB, Saxena SK (1992) A unified equation of state for fluids of C-H-O-N-S-Ar composition and their mixtures up to very high-temperatures and pressures. Geochim Cosmochim Acta 56:3611-3626

Bureau H, Keppler H (1999) Complete miscibility between silicate melts and hydrous fluids in the upper mantle: experimental evidence and geochemical implications. Earth Planet Sci Lett 165:187-196

Blundy JD, Falloon TJ, Wood BJ, Dalton JA (1995) Sodium partitioning between clinopyroxene and silicate melts. J Geophys Res 100:15501-15515

Bodinier J-L, Dupuy C, Dostal J (1988) Geochemistry and petrogenesis of Eastern Pyrenean peridotites. Geochim Cosmochim Acta 52:2893-2907

Bose K, Ganguly J (1995) Experimental and theoretical studies of the stabilities of talc, antigorite and phase A at high pressures with applications to subduction processes. Earth Planet Sci Lett 136:109-121

Boyd FR (1959) Hydrothermal investigations of amphiboles. *In:* Researches in Geochemistry Vol 1. Abelson PH (ed) Wiley, p 377-396

Boyd FR, Mertzman SA (1987) Composition and structure of the Kaapvaal lithosphere, South Africa. *In*: Magmatic Processes: Physiochemical Principles. Mysen B (ed) Geochemical Society Special Publication 1, p 13-24

Boyd FR (1990) Mantle metasomatism: evidence from a MARID-harzburgite compound xenolith. Carnegie Institution Washington Yearbook 90:18-23

Brandon AD, Draper DS (1996) Constraints on the origin of the oxidation state of mantle overlying subduction zones: An example from Simcoe, Washington, USA. Geochim Cosmochim Acta 60:1739-1749

Bryndzia LT, Wood BJ (1990) Oxygen thermobarometry of abyssal spinel peridotites: the redox state and the C-O-H volatile composition of the Earth's sub-oceanic upper mantle. Am J Sci 290:1093-1116

Bureau H, Keppler H (1999) Complete miscibility between silicate melts and hydrous fluids in the upper mantle: experimental evidence and geochemical implications. Earth Planet Sci Lett 165:187-196

Chazot G, Menzies MA, Harte B (1996) Determination of partition coefficients between apatite, clinopyroxene, amphibole, and melt in natural spinel lherzolites from Yemen: implications for wet melting of the lithospheric mantle. Geochim Cosmochim Acta 60:423-437

Cohen RE, O'Nions RK, Dawson JB (1984) Isotope geochemistry of xenoliths from East Africa: implications for development of mantle reservoirs and their interaction. Earth Planet Sci Lett 68:209-220

Conceicao RV, Green DH (2004) Derivation of potassic (shoshonitic) magmas by decompression melting of phlogopite+pargasite lherzolite. Lithos 72:209-229

Dawson JB, Smith JV (1977) The MARID (mica-amphibole-rutile-ilmenite-diopside) suite of xenoliths in kimberlite. Geochim Cosmochim Acta 41:309-323

Dawson JB, Smith JV (1982) Upper-mantle amphiboles: a review. Mineral Mag 45:35-46

Dawson JB (1984) Contrasting types of upper-mantle metasomatism? *In:* Kimberlites II: The mantle and Crust-Mantle Relationships. Kornprobst J (ed) Elsevier, pp 289-294

Dyar MD, Mackwell SJ, McGuire AV, Cross, LR, Robertson JD (1993) Crystal chemistry of $Fe^{3+}$ and $H^+$ in mantle kaersutite: implications for mantle metasomatism. Am Mineral 78:968-979

Edgar AD, Vukadinovic D (1992) Implications of experimental petrology to the evolution of ultrapotassic rocks. Lithos 28:205-220

Eggler DH (1978) The effect of $CO_2$ upon partial melting of peridotite in the system $Na_2O$-CaO-$Al_2O_3$-MgO-$SiO_2$-$CO_2$ to 35 kb, with an analysis of melting in a peridotite-$H_2O$-$CO_2$ system. Am J Sci 278:305-343

Elkins-Tanton LT, Grove TL (2003) Evidence for deep melting of hydrous metasomatized mantle: Pliocene high-potassium magmas from the Sierra Nevadas. J Geophys Res 108:2350, doi:10.1029/2002JB002168

Erlank AJ, Waters FG, Hawkesworth CJ, Haggerty SE, Allsopp HL, Rickard RS, Menzies M (1987) Evidence for mantle metasomatism in peridotite nodules from the Kimberley pipes, South Africa. *In*: Mantle Metasomatism. Menzies MA, Hawkesworth CJ (eds). Academic Press, p 313-361

Fabries J, Lorand J-P, Guiraud M (2001) Petrogenesis of the amphibole-rich veins from the Lherz orogenic lherzolite massif (Eastern Pyrenees, France): a case study for the origin of the orthopyroxene-bearing amphibole pyroxenites in the lithospheric mantle. Contrib Mineral Petrol 140:383-403

Field SW, Haggerty, SE, Erlank AJ (1989) Subcontinental metasomatism in the region of Jagersfontein, South Africa. *In*: Kimberlites and Related Rocks. Geol Soc Aust Spec Publ 14. Ross J (ed). Geological Society of Australia, p 771-784

Fleet ME (2003) Micas. The Geological Society

Foley S (1991) High-pressure stability of the fluor- and hydroxyl-endmembers of pargasite and K-richterite. Geochim Cosmochim Acta 55:2689-2694

Foley S (1992) Vein-plus-wall-rock melting mechanisms in the lithosphere and the origin of potassic alkaline magmas. Lithos 28:435-453

Frey FA, Prinz M (1978) Ultramafic inclusions from San Carlos, Arizona: petrological and geochemical data bearing on their petrogenesis. Earth Planet Sci Lett 38:129-176

Frost DJ, Fei Y (1998). Stability of phase D at high pressure and high temperature. J Geophys Res 103B:7463-7474

Frost DJ (1999) The stability of dense hydrous magnesium silicates in Earth's transition zone and lower mantle. *In* Mantle Petrology: Field Observations and High-Pressure Experimentation. Fei Y, Bertka CM, Mysen BO(ed) Geochemical Society, Special Publication No. 6, p 283-295

Frost DJ, Liebske C, Langenhorst F, McCammon CA, Tronnes RG, Rubie DC (2004) Experimental evidence for the existence of iron-rich metal in the Earth's lower mantle. Nature 428:409-412

Gilbert MC, Briggs DF (1974) Comparison of the stabilities of OH- and F-potassic richterites- a preliminary report. Trans Am Geophys Union 55:480-481

Gilbert MC, Helz RT, Popp RK, Spear FS (1982) Experimental studies of amphibole stability. Rev Mineral 9B: 229-353

Green DH (1973) Experimental melting studies on a model upper mantle composition at high pressure under water-saturated and water-undersaturated conditions. Earth Planet Sci Lett 19:37-53

Gregoire M, Lorand JP, O'Reilly SY, Cottin JY (2000) Armalcolite-bearing, Ti-rich metasomatic assemblages in harzburgitic xenoliths from the Kerguelen Islands: Implications for the oceanic mantle budget of high-field strength elements. Geochim Cosmochim Acta 64:673-694

Gregoire M, Bell DR, Le Roex AP (2003) Garnet lherzolites from the Kaapvaal craton (South Africa): trace element evidence for a metasomatic history. J Petrol 44:629-657

Gudmundsson G, Wood BJ (1995) Experimental tests of garnet peridotite oxygen barometry. Contrib Mineral Petrol 119:56-67

Halliday AN, Lee D-C, Tommasini S, Davies GR, Paslick CR, Fitton JG, James DE (1995) Incompatible trace elements in OIB and MORB and source enrichment in the sub-oceanic mantle. Earth Planet Sci Lett 133: 379-395

Harte B (1993) Mantle peridotites and processes- the kimberlite sample. In: Continental Basalts and Mantle Xenoliths. Hawkesworth CJ, Norry MJ (eds) Shiva, p 46-91

Hauri EH, Shimizu N, Dieu JJ, Hart SR (1993) Evidence for hotspot-related carbonatite metasomatism in the oceanic upper-mantle. Nature 365:221-227

Hawkesworth CJ, Erlank AJ, Marsh JS, Menzies MA, Van Calsteren P (1983) Evolution of the continental lithosphere: evidence from volcanics and xenoliths in southern Africa. *In*: Continental Basalts and Mantle Xenoliths. Hawkesworth MJ, Norry MJ (eds). Shiva, p 111-138

Hoal KEO, Hoal BG, Erlank AJ, Shimizu N (1994) Metasomatism of the mantle lithosphere recorded by rare earth elements in garnets. Earth Planet Sci Lett 126:303-313

Holloway JR (1973) The system pargasite $H_2O$-$CO_2$:a model for melting of a hydrous mineral with a mixed-volatile fluid. I. Experimental results to 8 kbar. Geochim Cosmochim Acta 37:651-666

Holloway JR (1987) Igneous fluids. Rev Mineral 17:211-233

Hübner SJ, Papike JJ (1970) Synthesis and crystal chemistry of sodium-potassium richterite $(Na,K)NaCaMg_5Si_8O_{22}(OH,F)_2$): a model for amphiboles. Am Mineral 55:1973-1992

Huckenholz HG, Gilbert MC, Kunzmann T (1992) Stability and phase relations of calcic amphiboles crystallized from magnesio-hastingsite compositions in the 1 to 45 kbar pressure range. N Jahr Miner Abh 164:229-268

Inoue T, Irifune T, Yurimoto H, Miyagi I (1998) Decomposition of K-amphibole at high pressures and implications for subduction zone volcanism. Phys Earth Planet Int 107:221-231

Ionov DA, Hofmann AW (1995) Nb-Ta-rich mantle amphiboles and micas: implications for subduction-related metasomatic trace element fractionations. Earth Planet Sci Lett 131:341-356

Ionov D (1998) Trace element composition of mantle-derived carbonates and coexisting phases in peridotite xenoliths from alkaline basalts. J Petrol 39:1931-1941

Irifune T, Kubo T, Isshiki M, Yamasaki Y (1998) Phase transformations in serpentine and transportation of water into the lower mantle. Geophys Res Lett 22:117-120

Jenkins DM (1983) Stability and composition relations of calcic amphiboles in ultramafic rocks. Contrib Mineral Petrol 83:375-384

Jones AP, Smith JV, Dawson JB (1982) Mantle metasomatism in 14 veined peridotites from Bultfontein Mine, South Africa. J Geol 90:435-453

Jones AP (1989) Upper mantle enrichment by kimberlitic or carbonatitic magmatism. *In*: Carbonates: Genesis and Evolutions. Bell K (ed) Unwin Hyman, p 448-463

Kanzaki M (1991) Stability of hydrous magnesium silicates in the mantle transition zone. Phys Earth Planet Inter 66:307–312

Kawamoto T, Leinenweber K, Hervig RL, Holloway JR (1995) Stability of hydrous minerals in $H_2O$-saturated KLB-1 peridotite up to 15 GPa. *In:* Volatiles in the Earth and Solar System. Farley KA (ed) American Institute of Physics, p 229-239

Kawamoto T (2004) Hydrous phase stability and partial melt chemistry in $H_2O$-saturated KLB-1 peridotite up to the uppermost lower mantle. Phys Earth Planet Int 143-144:387-395

Kawamoto T (2006) Hydrous phases and water transport in the subducting slab. Rev Mineral Geochem 62: 273-289

King PL, Hervig RL, Holloway JR, Vennemann TW, Righter K (1999) Oxy-substitution and dehydrogenation in mantle-derived amphibole megacrysts. Geochim Cosmochim Acta 63:3635-3651

Kinny PD, Compston JW, Bristow JW, Williams IS (1989) Archaean mantle xenocrysts in a Permian kimberlite: two generations of kimberlitic zircon in Jwaneng DK2, southern Botswana. *In*: Kimberlites and related rocks. Geol Soc Aust Spec Publ 14. Ross J (ed). Geological Society of Australia, p 833-842

Kinny PD, Meyer HOA (1994) Zircon from the mantle: a new way to date old diamonds. J Geol 102:475-481

Komabayashi T, Omori S, Maruyama S (2004) Petrogenetic grid in the system MgO-$SiO_2$-$H_2O$ up to 30 GPa, 1600 degrees C: Applications to hydrous peridotite subducting into the Earth's deep interior. J Geophys Res 109:Art. No. B03206

Konzett J, Sweeney RJ, Thompson AB, Ulmer P (1997) Potassium amphibole stability in the upper mantle: an experimental study in a peralkaline KNCMASH system to 8.5 GPa. J Petrol 38:537-568

Konzett J, Ulmer P (1999) The stability of hydrous potassic phases in lherzolitic mantle- an experimental study to 9.5 GPa in simplified and natural bulk compositions. J Petrol 40:629-652

Konzett J, Fei Y (2000) Transport and storage of potassium in the Earth's upper mantle and transition zone: an experimental study to 23 GPa in simplified and natural bulk compositions. J Petrol 41:583-603

Kushiro I (1970) Stability of amphibole and phlogopite in the upper mantle. Carnegie Inst Wash Year Book 68: 245-247

Kushiro I (1987) A petrological model of the mantle wedge and lower crust in the Japanese island arcs. *In*: Magmatic Processes: Physiochemical Principles. Geochem Soc Spec Publ 1. Mysen BO (ed) The Geochemical Society, p 165-181

Lambert IB, Wyllie PJ (1968) Stability of hornblende and a model for the low velocity zone. Nature 215:1240-1241

LaTourrette T, Hervig RL, Holloway JR (1995) Trace element partitioning between amphibole, phlogopite and basanite melt. Earth Planet Sci Lett 135:13-50

Leake BE, Woolley AR, Arps CES, Birch WD, Gilbert MC, Grice JD, Hawthorne FC, Kato A, Kisch HJ, Krivovichev VG, Linthout K, Laird J, Mandarino JA, Maresch WV, Nickel EH, Rock NMS, Schumacher JC, Smith DC, Stephenson NCN, Ungaretti L, Whittaker EJW, Guo YZ (1997) Nomenclature of amphiboles: Report of the subcommittee on amphiboles of the International Mineralogical Association, commission on new minerals and mineral names. Am Mineral 82:1019-1037

López Sánchez-Vizcaíno V, Trommsdorff V, Gómez-Pugnaire MT, Garrido CJ, Müntener O, Connolly JAD (2005) Petrology of titanian clinohumite and olivine at the high-pressure breakdown of antigorite serpentinite to chlorite harzburgite (Almirez Massif, S. Spain). Contrib Mineral Petrol 149:627-646

Luth RW (1995) Is phase A relevant to the Earth's mantle? Geochim Cosmochim Acta 59:679-682

Luth RW (1997) Experimental study of the system phlogopite-diopside from 3.5 to 17 GPa. Am Mineral 82: 1198-1209

Lykins RW, Jenkins DM (1992) Experimental determination of pargasite stability relations in the presence of orthopyroxene. Contrib Mineral Petrol 112:405-413

McCammon CA, Griffin WL, Shee SR, O'Neill HSC (2001) Oxidation during metasomatism in ultramafic xenoliths from Wesselton kimberlite, South Africa. Implications for the survival of diamond. Contrib Mineral Petrol 141:287-296.

McCammon C, Kopylova MG (2004) A redox profile of the Slave mantle and oxygen fugacity control in the cratonic mantle. Contrib Mineral Petrol 148:55-68

McInnes BIA, Gregoire M, Binns RA, Herzig PM, Hannington MD (2001) Hydrous metasomatism of oceanic sub-arc mantle, Lihir, Papua New Guinea: petrology and geochemistry of fluid-metasomatized mantle wedge xenoliths. Earth Planet Sci Lett 188:169-183

McNeil AM, Edgar AD (1987) Sodium-rich metasomatism in the upper mantle: implications of experiments on the pyrolite-$Na_2O$-rich fluid system at 950 °C, 20 kbar. Geochim Cosmochim Acta 51:2285-2294

Mancini F, Harlow GE, Cahill C (2002) The crystal structure and cation ordering of phase-X-$(K_{1-x-n})_2(Mg_{1-n}[Al,Cr]_n)_2Si_2O_7H_{2x}$: A potential K- and H-bearing phase in the mantle. Am Mineral 87:302-306

Matson DW, Muenow DW, Garcia MO (1986) Volatile contents of phlogopite micas from South African kimberlite. Contrib Mineral Petrol 93:399-408

Mengel K, Green DH (1989) Stability of amphibole and phlogopite in metasomatized peridotite under water-saturated and water-undersaturated conditions. *In*: Kimberlites and related rocks. Geol Soc Aust Spec Publ 14. Ross J (ed) Geological Society of Australia, p 571-581

Menzies MA, Murthy VR (1980) Nd and Sr isotope geochemistry isotope geochemistry of hydrous mantle nodules and their host alkali basalts: implications for local heterogeneities in metasomatically veined mantle. Earth Planet Sci Lett 46:323-334

Menzies MA, Rogers N, Tindle A, Hawkesworth CJ (1987) Metasomatic enrichment processes in lithospheric peridotites, an effect of asthenospheric-lithospheric interaction. *In*: Mantle Metasomatism. Menzies MA, Hawkesworth CJ (eds) Academic Press, p 313-361

Merrill RB, Wyllie PJ (1975) Kaersutite and kaersutite eclogite from Kakanui, New Zealand- water-excess and water-deficient melting to 30 kilobars. Geol Soc Am Bull 86:555-570

Michael PJ (1988) The concentration, behavior and storage of $H_2O$ in the sub-oceanic upper mantle: implications for mantle metasomatism. Geochim Cosmochim Acta 52:555-566

Millhollen GL, Irving AJ, Wyllie PJ (1974) Melting interval of peridotite with 5.7 percent water to 30 kilobars. J Geol 82:575-587

Miyagi I, Matsubaya O, Nakashima S (1998) Change in D/H ratio, water content and color during dehydration of hornblende. Geochem J 32:33-48

Modreski PJ, Boettcher AL (1972) Stability of phlogopite + enstatite at high pressure: A model for micas in the interior of the Earth. Am J Sci 272:852-869

Murayama JK, Nakai S, Kato M, Kumazawa M. (1986) A dense polymorph of $Ca_3(PO_4)_2$:a high pressure phase of apatite decomposition and its geochemical significance. Phys Earth Planet Int 44:293-303

Mysen BO, Boettcher AL (1975) Melting of a hydrous mantle: I Phase relations of natural peridotite at high pressures and temperatures with controlled activities of water, carbon dioxide, and hydrogen. J Petrol 16: 520-548

Mysen BO, Virgo D, Popp RK, Bertka CM (1998) The role of $H_2O$ in Martian magmatic systems. Am Mineral 83:942-946

Niida K, Green DH (1999) Stability and chemical composition of pargasitic amphibole in MORB pyrolite under upper mantle conditions. Contrib Mineral Petrol 135:18-40

Obata M (1980) The Ronda peridotite: garnet-, spinel- and plagioclase-lherzolite facies and the P-T trajectories of a high-temperature mantle intrusion. J Petrol 21:533-572

Obata M, Morten L (1987) Transformation of spinel lherzolite to garnet lherzolite in ultramafic lenses of the Austridic crystalline complex, northern Italy. J Petrol 28:599-623

O'Hara MJ, Mercy ELP (1963) Petrology and petrogenesis of some garnetiferous peridotites. Trans Royal Soc Ed 65:251-314

O'Neill HStC, Rubie DC, Canil, D, Geiger CA, Ross CR, Seifert F, Woodland AB (1993) Ferric iron in the upper mantle and in transition zone assemblages: Implications for relative oxygen fugacities in the mantle. Geophys Monograph 74 IUGG 14:73-89

O'Reilly SY, Griffin WL (2000) Apatite in the mantle: implications for metasomatic processes and high heat production in Phanerozoic mantle. Lithos 53:217-232

O'Reilly SY, Griffin WL (1988) Mantle metasomatism beneath western Victoria, Australia: I. Metasomatic processes in Cr-diopside lherzolites. Geochim Cosmochim Acta 52:433-447

Ohtani, E, Shibata T, Kubo T, Kato T (1995) Stability of hydrous phases in the transition zone and the upper most part of the lower mantle. Geophys Res Lett 22:2553-2556

Popp RK, Virgo D, Yoder HS, Hoering TC, Phillips MW (1995) An experimental study of phase equilibria and Fe oxy-component in kaersutitic amphibole: implications for the $f_{H2}$ and $a_{H2O}$ in the upper mantle. Am Mineral 80:534-548

Righter K, Dyar MD, Delaney JS, Vennemann TW, Hervig RL, King PL (2002) Correlations of octahedral cations with $OH^-$, $O^{2-}$, $Cl^-$ and $F^-$ in biotite from volcanic rocks and xenoliths. Am Mineral 87:142-153

Robinson P, Spear FS, Schumacher JC (1982) Phase relations of metamorphic amphiboles: natural occurrence and theory. Rev Mineral 9B:1-227

Roden MF, Murthy R (1985) Mantle metasomatism. Ann Rev Earth Planet Sci 13:269-296

Ryabchikov ID, Boettcher AL (1980) Experimental evidence at high pressure for potassic metasomatism in the mantle of the Earth. Am Mineral 65:915-919

Sato K, Katsura T, Ito E (1997) Phase relations of natural phlogopite with and without enstatite up to 8 GPa: implication for mantle metasomatism. Earth Planet Sci Lett 146:511-526

Scambelluri M, Hermann J, Morten L, Rampone E (2006) Melt- versus fluid-induced metasomatism in spinel to garnet wedge peridotites (Ulten Zone, Eastern Italian Alps): clues from trace element and Li abundances. Contrib Mineral Petrol 151:372-394

Schmidt MW, Poli S (1998) Experimentally based water budgets for dehydrating slabs and consequences for arc magma generation. Earth Planet Sci Lett 163:361-379

Schmidt MW, Vielzeuf D, Auzanneau E (2004) Melting and dissolution of subducting crust at high pressures: the key role of white mica. Earth Planet Sci Lett 228:65-84

Schneider ME, Eggler DH (1986) Fluids in equilibrium with peridotite minerals: implications for mantle metasomatism. Geochim Cosmochim Acta 50:711-724

Schrauder M, Navon O (1994) Hydrous and carbonatitic mantle fluids in fibrous diamonds from Jwaneng Botswana. Geochim Cosmochim Acta 58:761-771

Seyler M, Mattson PH (1989) Petrology and thermal evolution of the Tinaquillo peridotite (Venezuela). Journal Geophys Res 94:7629-7660

Shaw CSJ, Eyzaguirre J (2000) Origin of megacrysts in the mafic alkaline lavas of the West Eifel volcanic field, Germany. Lithos 50:75-95

Shen AH, Keppler H (1997) Direct observation of complete miscibility in the albite-$H_2O$ system. Nature 385: 710-712

Shieh SR, Mao HK, Hemley RJ, Ming LC (1998) Decomposition of phase D in the lower mantle and the fate of dense hydrous silicates in subducting slabs. Earth Planet Sci Lett 159:13-23

Shimizu N (1975) Rare earth elements in garnets and clinopyroxenes from garnet lherzolite nodules in kimberlites. Earth Planet Sci Lett 25:26-32

Sweeney RJ, Thompson AB, Ulmer P (1993) Phase relations of a natural MARID composition and implications for MARID genesis, lithospheric melting and mantle metasomatism. Contrib Mineral Petrol 115:225-241

Sudo A, Tatsumi Y (1990) Phlogopite and K-amphibole in the upper mantle: implication for magma genesis in subduction zones. Geophys Res Lett 17:29-32

Tatsumi Y, Hamilton DL, Nesbitt RW (1986) Chemical characteristics of fluid phase released from a subducted lithosphere and origin of arc magmas: evidence from high pressure experiments and natural rocks. J Volcanol Geotherm Res 29:293-310

Taylor WR, Green DH (1988) Measurement of reduced peridotite-C-O-H solidus and implications for redox melting of the mantle. Nature 332:349-352

Thibault Y, Edgar AD, Lloyd FE (1992) Experimental investigation of melts from a carbonated phlogopite lherzolite: implications for metasomatism in the continental lithospheric mantle. Am Mineral 77:784-794

Tiepolo M, Vannucci R, Oberti R, Foley S, Bottazzi P, Zanetti A (2000) Nb and Ta incorportation and fractionation in titanian pargasite and kaersutite: crystal-chemical constraints and implications for natural systems. Earth Planet Sci Lett 176:185-201

Thompson AB (1992) Water in the Earth's upper mantle. Nature 358:295-302

Thompson JB, Laird J, Thompson AB (1981) Reactions in amphibolite, greenschist and Blueschist. J Petrol 23: 1-27

Trønnes RG, Edgar AD, Arima M (1985) A high pressure-high temperature study of $TiO_2$ solubility in Mg-rich phlogopite: implications to phlogopite chemistry. Geochim Cosmochim Acta 49:2323-2329

Trønnes RG (2002) Stability range and decomposition of potassic richterite and phlogopite end members at 5-15 GPa. Mineral Petrol 74:129-148

Ulmer P, Trommsdorff V (1999) Phase relations of hydrous mantle subducted to 300 km. *In* Mantle Petrology: Field Observations and High-pressure Experimentation. Fei Y, Bertka CM, Mysen BO (ed) Geochemical Society, Special Publication No. 6, p 259-281

Ulmer P (2001) Partial melting in the mantle wedge - the role of $H_2O$ in the genesis of mantle-derived 'arc-related' magmas. Phys Earth Planet Int 127:215-232

van Achterbergh E, Griffin WL, Stiefenhofer J (2001) Metasomatism in mantle xenoliths from the Letlhakane kimberlites: estimation of element fluxes. Contrib Mineral Petrol 141:397-414

Wagner C, Deloule E, Mokhtari A (1996) Richterite-bearing peridotites and MARID-type inclusions in lavas from North Eastern Morocco: mineralogy and D/H isotopic studies. Contrib Mineral Petrol 124:406-421

Wallace ME, Green DH (1988) An experimental determination of primary carbonatite magma composition. Nature 335:343-346

Wallace ME, Green DH (1991) The effect of bulk rock composition on the stability of amphibole in the upper mantle: implications for solidus positions and mantle metasomatism. Mineral Petrol 44:1-19

Wallace PJ (1998) Water and partial melting in mantle plumes: Inferences from the dissolved $H_2O$ concentrations of Hawaiian basaltic magmas. Geophys Res Lett 25:3639-3642

Waters FG (1987) A suggested origin of MARID xenoliths in kimberlites by high pressure crystallization of an ultrapotassic rock such as lamproite. Contrib Mineral Petrol 95:523-533

Watson BE (1980) Apatite and phosphorus in mantle source regions: an experimental study of apatite/melt equilibria at pressures to 25 kbar. Earth Planet Sci Lett 51:322-335

Weiss M (1997) Clinohumites: a field and experimental study. ETH Dissertation No. 12202, 168 pp.
Wilkinson JFG, Le Maitre RW (1987) Upper mantle amphiboles and micas and $TiO_2$, $K_2O$ and $P_2O_5$ abundances and $100Mg/(Mg+Fe^{2+})$ ratios of common basalts and andesites: implications for modal mantle metasomatism and undepleted mantle compositions. J Petrol 28:37-73
Wilshire HG, Shervais JW (1975) Al-augite and Cr-diopside ultramafic xenoliths in basaltic rocks from Western United States. Phys Chem Earth 9:257-276
Witt-Eickschen G, Seck HA, Reys CH (1993) Multiple enrichment processes and their relationships in the subcrustal lithosphere beneath the Eifel (Germany). J Petrol 34:1-22
Witt-Eickschen G, Kramm U (1998) Evidence for the multiple stage evolution of the subcontinental lithospheric mantle beneath the Eifel (Germany) from pyroxenite and composite pyroxenite/peridotite xenoliths. Contrib Mineral Petrol 131:258-272
Woermann E, Rosenhauer M (1985) Fluid phases and the redox state of the earths mantle. Fortschr Mineral 63: 263-349
Wood BJ, Bryndzia LT, Johnson KE (1990) Mantle oxidation state and its relationship to tectonic environment and fluid speciation. Science 248:337-345
Woodland AB, Kornprobst J, McPherson E, Bodinier J-L, Menzies MA (1996) Metasomatic interactions in the lithospheric mantle: petrologic evidence from the Lherz massif, French Pyrenees. Chem Geol 134:83-112
Woodland AB, Koch M (2003) Variation in oxygen fugacity with depth in the upper mantle beneath the Kaapvaal craton, South Africa. Earth Planet Sci Lett 214:295-310
Wyllie PJ (1978) Mantle fluid compositions buffered in peridotite-$CO_2$-$H_2O$ by carbonates, amphibole, and phlogopite. J Geol 86:687-713
Yang HX, Konzett J, Prewitt CT (2001) Crystal structure of Phase X, a high pressure alkali-rich hydrous silicate and its anhydrous equivalent. Am Mineral 86:1483-1488
Yang H-J, Frey FA, Clague DA (2003) Constraints on the source components of lavas forming the Hawaiian North Arch and the Honolulu volcanics. J Petrol 44:603-627
Yaxley GM, Green DH, Kamenetsky V (1998) Carbonatite metasomatism in the southeastern Australian lithosphere. J Petrol 39:1917-1930
Yoder HS, Kushiro I (1969) Melting of a hydrous phase: phlogopite. Am J Sci 267A: 558-582
Young ED, Virgo D, Popp RK (1997) Eliminating closure in mineral formulae with specific application to amphiboles. Am Mineral 82:790-806
Zanetti A, Mazzucchelli M, Rivalenti G, Vannucci R (1999) The Finero phlogopite-peridotite massif: an example of subduction-related metasomatism. Contrib Mineral Petrol 134:107-122